SAPIENZA
Università di Roma
Facoltà di Scienze Matematiche Fisiche e Naturali

DOTTORATO DI RICERCA
IN GENETICA E BIOLOGIA MOLECOLARE

XXXII Ciclo
(A.A. 2018/2019)

Functional characterization of FUS-dependent circular RNAs in physiological and pathological conditions

Eleonora D'Ambra

Docente guida
Prof. Irene Bozzoni

Tutore
Prof. Mariangela Morlando

Coordinatore

Prof. Fulvio Cruciani

SUMMARY

The RNA binding protein FUS participates in several RNA biosynthetic processes; it controls alternative splicing in the nervous system and has recently been demonstrated to be involved in circular RNA (circRNA) biogenesis, a new class of covalently closed RNA molecules arising from a backsplicing event. Notably, alterations of RNA splicing due to FUS mutations have been linked to the pathogenesis of Amyotrophic Lateral Sclerosis (ALS), a neurodegenerative disease that affects upper and lower motoneurons (MNs). In order to investigate the role played by circRNAs in a neuronal system and their potential involvement in ALS, we focused on two circRNAs, circ-31 and circ-16. These circRNAs are conserved between human and mouse, upregulated during neuronal differentiation and highly expressed in MNs, moreover, their expression is affected in FUS-KO MNs and in MNs carrying the P517L FUS mutation. The latter causes a relevant FUS delocalization in the cytoplasm, which is linked to one of the most severe forms of familial ALS where the mutant protein forms cytoplasmic aggregates. *In situ Hybridization* and immuno-fluorescence approaches showed that circ-31 and circ-16 are localized in the cell body as well as in neuronal processes both in WT and FUS mutant MNs. Oxidative stress on MNs induces stress granule (SG) formation and in mutant cells this was used to mimic pathological ALS conditions where FUS aggregates mostly colocalize with SGs. In this condition, circ-31 is retained in the cell body, and in FUS mutant MNs, tend to co-localize with FUS-positive SG in a preferential manner when compared to circ-16. This suggests an active role of mutant FUS granules in trapping this transcript. Moreover, in order to study circRNA function in physiological MN conditions, we set up and performed RNA pull down experiments in *in vitro*-derived MNs by using antisense biotinylated oligonucleotides and UV and AMT-psoralen derivative crosslinking, in order to look at protein and RNA interactors respectively. Data from these experiments are currently under analysis. In parallel, we set up a CRISPR/Cas9 approach in order to obtain circRNA KO.

INDEX

1. INTRODUCTION

1.1 The origin of the non-coding world

"DNA makes RNA, RNA makes Protein". In 1958 Francis Crick enounced the central dogma of Molecular Biology, describing the flow of genetic information which passes through RNA molecules, from genes to proteins that were considered to be the main actors in cellular processes. Indeed, in 1961 the messenger RNA (mRNA) was finally discovered, a very unstable form of RNA characterized by the presence of 7-methylguanosine at 5' (CAP) and polyA (adenosine) tail at 3'[1] [2]. In the same year Jacob and Monod[2] established for the first time the concept of mRNA as the intermediate molecule connecting genetic information and protein synthesis. During the '70s other species of RNAs were rapidly discovered, such as tRNA and rRNA. Although don't codifying for protein, since lacking in a CAP and PolyA tail, these last class of RNAs are involved in the complexity of protein translation mechanism, encouraging the protein-centre view of molecular biology at the time.
In 1982 Thomas Cech showed that RNA has a catalytic function, demonstrating that self-splicing or self-cleaving RNAs can make single cuts, carrying out a protein-independent catalysis[3], and in 1989 he was awarded with the Nobel Prize for the discovery of the ribozyme. Later in the '90s, with the discovery of the H19 and Xist transcripts, a new category of RNAs began to arise, the long-non coding RNAs. A few years later microRNAs also were discovered[4] and in 1998, Fire and Mello published the RNA interference mechanism, based on RNA-RNA interactions[5], a discovery which allowed them to earn the Nobel Prize. The idea that a non-coding RNA might have a proper function, not related to protein translation, was gaining popularity as the number of new and putative functional ncRNAs kept expanding[6] [7] [8]. The Human genome project was concluded in 2003 and together with the Encyclopaedia of DNA Elements (ENCODE) project, was likely the final proof that something else besides coding genes and proteins was of great importance in cells; the world of molecular biology could not be protein-centric any longer. Indeed, the ENCODE project provided a complete view of regions of transcription, transcription factor

occupancy and chromatin dynamics of the human genome, showing that 80.4% of it participates in at least one biochemical RNA and/or chromatin-associated event, in at least one cell type. Most of the genome is transcribed, but only 2.94 % of the genome is protein-coding; the rest was considered "junk"[9] [10]. The unavoidable question is the following: why should a cell consume energy and space for something that is not useful? In the last two decades, Molecular Biologists wanted to answer this question, focusing their attention on RNA in order to unveil all the potential functions of non-coding RNAs and to understand whether they bear any biological function.

1.2 Characteristic and general function of ncRNAs

Non-coding RNAs are abundant transcripts in all cells and are classified according to their molecular characteristics. Besides the most famous and well-known t-RNAs and rRNAs, we recognize many classes of ncRNAs and classify them depending on their length, shape and localization. Among the most studied and characterised ncRNAs there are: microRNAs (miRNAs) that are 19-20 nucleotide (nt) long and mainly localise in the cytoplasm; piwi-RNAs (pi-RNA), 23-26 nt nuclear RNAs[11]; small-nuclear and small nucleolar RNAs (snRNA and snoRNA) involved with the splicing machinery[12] and finally, long non-coding RNAs (lncRNAs) that are longer than 200 nt and can localise both in the cytoplasm and nucleus.[13] Most recently, a new class of lncRNAs has been discovered, the so-called circular RNAs (circRNAs).
Although most of ncRNA classes have a known role in cellular processes, lncRNA and circRNA have been considered non-functional for long time. LncRNAs, in particular, were thought to be transcripts produced from an aberrant transcription machinery that gave rise to "transcriptional noise"[14]. One of the first pieces of evidence regarding the functional importance of lncRNAs in biological processes was the discovery of Xist, and its importance for X-chromosome inactivation[15][16]. Many other different lncRNAs have been discovered in the last two decades, and interest was focused on nuclear lncRNAs, considered important players in gene expression regulation. Indeed, these molecules serve as chromatin structure

modifier acting as nuclear architects through DNA or protein interaction[8]. The involvement of nascent RNAs, and ncRNAs, in chromatin remodelling was previously demonstrated with nucleoli. In these nuclear compartments rRNA-coding genes, which are spread and transcribed from five chromosomes, are spatially organized in domains. These domains lose their organisation if digesting or stopping the production of RNA, but not blocking protein synthesis, meaning a strong reliance of nucleoli architecture on rRNA transcription[8] . Similarly, many lncRNAs have been found to be involved in chromatin remodelling processes and in nuclear domain formation and maintenance. One example is NEAT1, which is a key player for the formation of heterochromatin[17], essential for the maintenance of paraspeckles. MALAT1 is another example, involved in the regulation of oncogene expression and present in nuclear speckles; ribonucleoparticles where actively transcribed genes are included[8] [18]. In other cases, lncRNAs act as enhancer, allowing the interaction of a transcription factor with the DNA, such as LED which allows p53 activity.

If the nuclear localisation of ncRNA permits the interaction with DNA and RNA/DNA-BP, the cytoplasmic localisation as well would permit the interaction with RNAs and RNA binding proteins (RBP). Many different functions are attributed to cytoplasmic ncRNAs; the interaction of lncRNA with RBP can favour mRNA stability such as in the case of TINCR-STAU1 lncRNP. TINCR-mRNA interaction occurs through a 25-nucleotide motif (TINCR box) in interacting mRNAs and the direct binding among TINCR and Staufen1 protein (STAU1) seems to be involved in mRNA stabilisation, such as KRT80[19]. Alternatively, in the case of lncRNA BACE1-AS (BACE1 antisense) the lncRNA itself is able to stabilize the mRNA BACE1(the β-site amyloid precursor protein (APP)-cleaving enzyme) through a region of partial complementarity, following exposure to various cell stressors[20], and BACE1-AS is in turn stabilized by HuR[21]. LncRNA can also mediate mRNA Decay as the 1/2-sbsRNAs-STAU1complex, where a STAU1-mediated decay target can form STAU1-binding sites by imperfect base-pairing between an Alu element in its 3' UTR and another Alu element in a cytoplasmic, polyadenylated long non-coding RNA (lncRNA).[22] The very interesting aspect of ncRNAs in the cytoplasm is the fine

network that different RNA molecules have established so as to regulate post-transcriptional events, as it occurrs in miRNA/mRNA and competing endogenous RNA (ceRNA) axis. miRNAs are among the most abundant ncRNAs in cells[10]. These incredible small RNA molecules are important gene expression regulators. An imperfect match between a miRNA, bound to AGO2 protein, and the mRNA target, induces mRNA translational repression and eventually mRNA degradation through the cross-talk between the RISC complex and PABP2/CCR4-NOT1[23]. Cytoplasmic lncRNAs can compete with the mRNA for miRNA binding and sequester the miRNAs. This mechanism resumes mRNA translation and increases its stabilisation. One example of cytoplasmic lncRNA described as competing endogenous RNA is linc-MD1, that by binding miR133 and miR135 positively regulates the expression of two transcription factors involved in muscle differentiation[24]. The network established between RNA molecules prompted the study of cytoplasmic circRNAs. In this context, Hansen and co-workers discovered that the first circRNA to be identified, CDR1as, functions as a ceRNA. They found that CDR1as has 70 binding sites for miR-7 and was thus defined as a sponge for this miRNA[25]. However, the gene expression profiling in CDR1as KO mice suggested that this circRNA could be a carrier/stabiliser for mir-7 rather than a sponge [26]. Moreover, CDR1as has an additional binding site for mir-671 but in this case the perfect complementarity between circRNA and miRNA determines the degradation of CDR1as. With regards to CDR1as as a carrier, the miR-671-mediated degradation may be a way to release the miR-7 cargo.

1.3 CircRNAs

CircRNAs are a class of newly rediscovered ncRNAs, characterised by a specific circular shape. The existence of the circular form of RNA was originally discovered by Sanger in 1976 when he identified viroids[27] . Lately, in 1986, Kos identified the viroid HDV (Hepatitis delta virus) a single stranded RNA genome virus, satellite of HBV (Hepatitis B virus) which is able to infect human cells[28]. Circular RNA molecules were observed during the tRNAs[29][30] and rRNAs[31] [32] 16S and 23S processing reactions of some archaea. In other cases, circular RNA molecules can arise from intron (group I or II) excision during splicing reactions, leading to the formation of circular intron RNAs (ciRNAs) that may also be functional, and the first example was the ciRNA arising from the rRNA of Tetrahymena[33] through autocatalytic ribozyme action [34]. Other well-known ciRNAs arise from group II introns, that are self-splicing ribozymes found in bacteria and eukaryotic organelles, they are intron-lariat ciRNA with a 2'-5' bond. Similar products are found during eukaryotic canonical splicing reactions when the intron lariats resulted resistant to debranching activity[35]. Despite ciRNA function being still under study, some features suggest a role in enhancing the transcription of their resident genes. Indeed, are retained in the nucleus, close to their transcription site, and their knock down causes the downregulation of the host gene's mRNA expression, in addition they have been shown to act in cis by modulating RNA polymerase II[36].
The exonic circRNA where instead initially identified in 1991, when Nigro and colleagues[37] discovered a circRNA arising from the DCC (Deleted in Colorectal Carcinoma) tumour suppressor gene; initially this circRNA was considered an error of the splicing mechanism. Few years later, in 1993, Cocquerelle and co-workers identified a highly stable circRNA with a half-life of 48 hours, arising from the EST-1 gene and having a 3'-5' phosphodiester bond at the junction site[38]. In the same year an *"RNA with unusual structure, with 3' sequences located in a 5' position"* was found as the most highly expressed transcript in mice testis and arising from the Sry gene, which is responsible for sex specification in mammals. 90% of Sry transcripts give rise to this mono exonic circRNA that localises in the cytoplasm and is not able to code for proteins[39].The real opportunity

for the recognition of the abundance of circRNA in plants[40], archaea[32] and eukaryotes[41] came with the Omics-era. With the high-throughput technologies[42], scientists could finally look at the whole cell transcriptome and in 2012 Salzman and colleagues identified hundreds of human genes generating circRNAs[41]. An incredible number of circRNAs in different cell types have rapidly been discovered and nowadays the emphasis has shifted towards finding circRNA functions, a new goal for molecular biology.

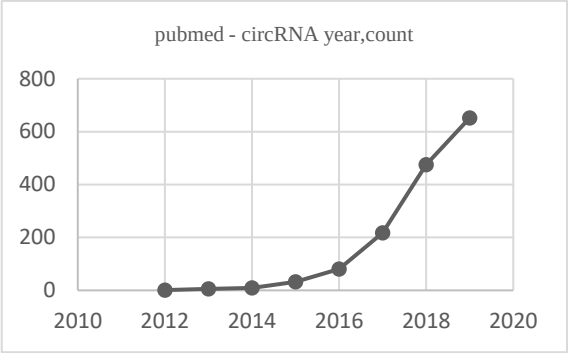

PubMed resource: circRNA publications since the RNA sequencing approach was introduced.

1.4 Molecular characteristics, biogenesis and function of circRNAs

The characteristic circular shape of circRNAs is due to the phosphodiester bond, between a donor 5' splice site downstream and an acceptor 3'splice site upstream, generated by a non-canonical splicing reaction. Therefore, those molecules lack 3' and 5' termini, characteristic of linear RNAs, and lack the CAP and polyA, typical of mRNAs and needed for translation mechanism. Circular shape contributes to circRNAs famous stability, (≈48 hours)[43], which is much longer than the average half-life of mRNAs, (≈10 hours[44]) and this is probably related to the resistance to RNA-exonuclease activity, such as RNase R. Interestingly, this enzyme is also applied to experimentally validate the circularity of circRNAs[41 45], excluding artefact molecules generated by high-throughput approach.
The dual destiny of a pre-mRNA depends on splicing activity. Nascent pre-mRNAs can be processed through a canonical splicing mechanism producing mRNA, or can undergo a non-canonical mechanism, that produces circRNAs. In some cases the two mechanisms can compete with each other and the spliceosome may prefer one of the two mechanisms[46]. So far, there is no evidence concerning the co-expression of circRNA and mRNA lacking the circRNA-included exons[43 47 41]. Even though circRNA biogenesis relies on a non-canonical splicing mechanism, it requires the canonical spliceosome[46 48] and three mechanisms have been described to favour RNA molecule circularisation: the "exon skipping" [49]; the "direct backsplicing" [50]and the "debranching resistant intron lariat". This last mechanism is known to generate intron lariat circular RNAs, the ciRNAs described above. Although highly enriched in mammalian cells, ciRNAs must be considered different to circRNAs since they contain intronic sequences, and they involve a 2′–5′ phosphodiester linkage at the branch point[36].
The most accredited mechanism is the direct backsplicing that, despite not being fully elucidated yet, suggests that introns flanking the RNA region involved in the circRNA are key players of the circularisation process. Such introns are characterised by their long length, as well as encompassing inverted repeated sequences [43 51] and/or RBP binding sites that allow the circularisation of the linear

molecule[46] [51] [52]. Inverted sequences were initially thought to be important for the circularisation from the discovery of circSry in 1993[39] [53]; lately Jeck and co-workers, [43] with the genome-wide analysis, confirmed the presence of complementary inverted sequences, in particular of ALU repeats and a representative scheme adapted from Zhang and co-workers is showed in figure 1.

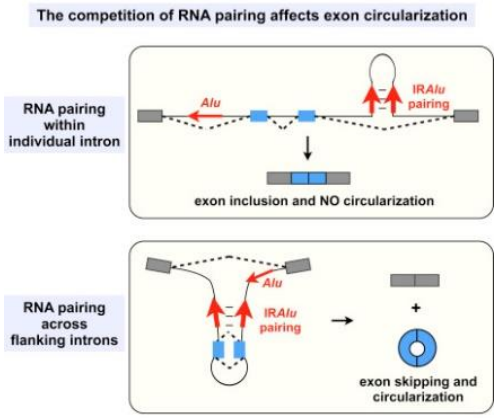

Figure 1: CircRNA circularization mediated by flanking introns (adapted from Zhang et al., Cell 2014) [52]

The involvement of complementary sequences in introns was shown to be a hallmark for the prediction of circRNA biogenesis; indeed, Ivanov and co-workers[54] showed that circRNA-flanking introns lead to the circularisation through RNA-RNA interactions and that those may be edited and compromised by the ADAR1 enzyme, known to target dsRNAs (Adenosine to inosine editing). Nonetheless, ADAR1 is not the only protein involved in circRNA biogenesis, indeed, as mentioned above, flanking introns can contain sites for RBP binding. While ADAR1 is a negative regulator of circRNA biogenesis, one well studied example for an RBP enhancer of circularisation is the splicing factor MuscleBlind (MBL) in Drosophila, able to bind introns flanking the second exon that generates circMBL[46]. The authors also show that canonical and back splicing events compete

with each other: a strong increase of MBL mRNA and protein induces an upregulation of circRNA biogenesis and a switch from linear splicing to the circular one. In mammalian cells, two other proteins have been demonstrated to be involved in circRNA biogenesis: Quaking (QKI), that binds flanking introns and induces the circularisation through its dimerization[55]; and Fused in Sarcoma (FUS), that was studied in our lab[56] (Fig.2).

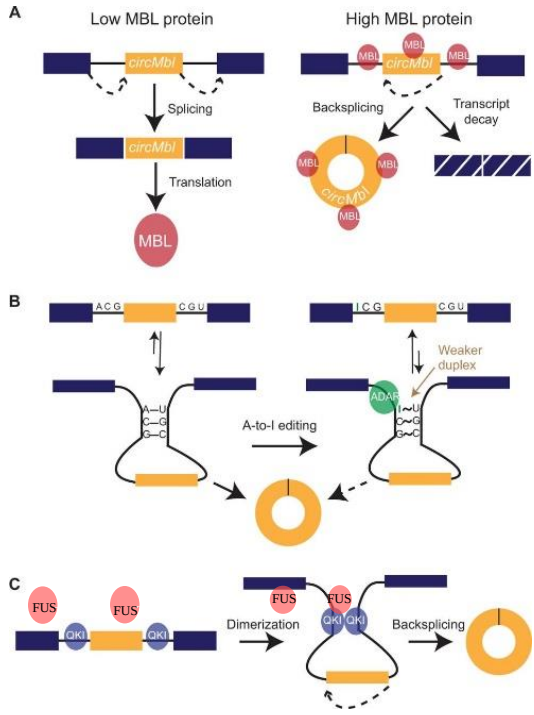

Figure 1: circRNA biogenesis (adapted from Barrett and Salzman 2016)[57]

Hitherto, few examples of circRNA functions have been demonstrated, despite the many hypotheses regarding putative roles. The highly tissue-specific abundance of circRNAs, in particular in brain [58 59], the good inter-species conservation (5-23% depending on the species) and the dynamic expression during embryonic development[60 61 49] all strengthen the idea that circRNAs might carry out important roles in biological processes. Alike lncRNAs, circRNAs can localise in the nucleus or cytoplasm, widely depending

on their structure[62]; and a different localisation suggests a different function. Exon-circRNAs (ecircRNAs), that in mammalian cells are the mostly expressed ones[47], are usually exported to the cytoplasm, probably via the exon junction complex (as for mRNAs), albeit, so far, only the Hel25E factor in *Drosophila* and its human homologs UAP56/URH49 are demonstrated to be involved in nuclear export of mature circRNAs[63]. Dissimilarly, intron-retained circRNAs (EIcircRNAs) are confined into the nucleus as well as ciRNAs. Nuclear circRNA, as well as some lncRNAs are able to regulate host gene transcription. EIcircRNAs, such as circPAIP2 and circEIF3J are associated to Polymerase II (PolII), U1A and U1C proteins and U1 small nuclear RNA, and are involved with the engagement of the transcription complex on the host gene promoter, through an RNA-RNA interaction with U1 snRNA[64]. The ciRNA, ci-ankrd52, can interact with PolII and modulate its transcriptional activity[36]. Given this involvement in transcriptional regulation, it would be interesting to investigate whether circRNAs, as other lncRNAs, might also have other roles, such as the engagement of transcription factors or epigenetic factors in a specific region of the DNA[8]. The majority of circRNAs expressed in mammals are cytoplasmic and are composed by exons,[65] and are particularly enriched in the neuronal axoplasm and at the synaptic level[58] [66] [25]. In contrast to neural tissues, in actively proliferating cells such as cancer cells, circRNAs are downregulated, possibly because fast cell division dilutes the number of molecules before reaching steady-state levels[67]. Circ-FOXO3 and circ-ZNF609, for instance, are regulators of cell proliferation by inhibiting or promoting, respectively, the proteasome mediated degradation of specific cell cycle-related proteins[68] [69] and circ-ZNF609, was described to be upregulated in in rhabdomyosarcoma[69]. The most famous and best-characterized circRNA, CDR1as (cerebellar degeneration-related antigen 1-antisense circRNA) is an effective example of circRNA function in the cytoplasm, being a sponge for miRNAs. Hansen and colleagues in 2011 found out that CDR1as was enriched in both mouse and human brain, and could be targeted by miR-671 that, due to the perfect complementarity, was able to induce the degradation of CDR1as[70]. That was the first example of circRNA degradation through the miR/AGO2 mechanism[70]. In 2013, the same group demonstrated that not only

was CDR1as targeted by miR-671, but it also contained 77 binding sites for miR-7[25]. In this case the interaction was based on non-perfect complementarity, therefore CDR1as was supposed to be a sponge able to sequester miR-7 from its mRNA targets, in a similar manner as described for competing endogenous lncRNAs[24]. In 2017, Piwecka and co-workers demonstrated that CDR1as could be involved in the stabilization or transport of miR-7 and that this mechanism is important for sensorimotor gating and synaptic transmission. Confirming the foregoing, in CDR1as KO mice, miR7 and miR671 expression levels were altered due to post-transcriptional deregulation in absence of CDR1as. Indeed, miR7 and miR671 mRNA targets were found to be altered in CDR1as KO mice[26]. CDR1as is expressed in hundreds of copies in neuronal soma and neurites and contains a large number of miRNA binding sites. Other circRNAs have been thought to function through a sponge mechanism but besides CDR1as, none have such a considerable number of binding sites for a miRNA. For instance, another sponge circRNA is circSry that contains 16 binding sites for miR-138[25], which are less compared to CDR1a.When addressing the putative role of a circRNA as a sponge, it is important to consider the stoichiometric ratio among the circRNA and the miRNA molecules that are known to be highly abundant while the majority of circRNA described as miRNA sponge have only one or very few binding site, raising the doubt regarding the effectiveness of sponge activity[71].
CircRNAs can also interact with proteins and they may sequester them from other targets, as shown for circMBL that via its binding to the MBL protein in the cytoplasm maintains an equilibrium that favours the accumulation of the linear MBL mRNA [46]. Moreover they can act as a scaffold for proteins, as in the case of circFOXO3 that interacts with mouse double-minute 2 (MDM2) and p53 thus favouring the MDM2-dependent ubiquitylation of p53[68]. Very recently, an interesting additional role for circRNAs has been discovered that is based on their 3D structures. Liu and co-workers showed that a cohort of circRNAs, sharing 16-26 bp intra-double stranded RNA regions, can bind PKR, a dsRNA activated protein kinase. This interaction is affected upon viral infection, when RNAase L is activated and degrades circRNAs, a process that is required for PKR activation in the early stage of the innate immune

response and that is linked to the autoimmune disease systemic lupus erythematosus[72]. Most circRNAs originate from the second exon of the pre-mRNA or at least from the initial exons, meaning that they could contain the AUG [73]. However, among them, a few circRNAs have been demonstrated to code for small peptides[46 74 75]. Studies with a reporter plasmid containing IRES upstream circRNAs sequence with an infinite open reading frame (ORF) produced proteins, revealing that human circRNAs contain extensive m^6A modifications. This was shown to promote cap-independent circRNA translation through the involvement of the reader protein YTHDF3 and the IRES-specialised translation initiation factor eIF4G2 [76]. One example of m^6A-related circRNA translation is circE7, a circRNA originating from the HPV16 E7 oncoprotein coding gene[77].

1.5 CircRNAs in the Brain

Despite circRNAs being expressed in different tissues, their expression levels change depending on the tissue and cells characteristics. For instance, in proliferating cells, the high rate of cell division could dilute circRNAs concertation in the cells, a phenomenon that does not occur in neurons, which are post mitotic cells. This could be one of the reasons why circRNAs have been demonstrated to be more highly expressed in the brain and nervous system when compared with other tissues[41 66 46]. Nonetheless, the specificity of circRNA expression and localization suggest a more appropriate reason related to the enrichment of circRNAs in the brain, and nowadays a lot of effort is dedicated to unveiling the role of these molecules in the complexity of the neuronal system. You and co-workers demonstrated that most of the circRNAs expressed in the hippocampus arise from genes involve in brain function or development. Precisely, in postnatal mice (P10), up-regulated circRNAs arise from genes involved in synapse development and plasticity. Although most circRNAs show expression patterns that are compatible with the expression levels of their linear host genes, some circRNAs such as circRims2, circEl2 and circDym, are expressed in specific regions of the brain and show an expression level trend that is unrelated to the linear counterpart's [59]. Moreover, the same group demonstrated that homeostatic plasticity using bicuculline, an antagonist of the GABA-A receptor, could induce circHomer transcription, showing an increased level of the molecule both in soma and in neurites. Interestingly, circRNAs can also localise differently to their linear counterparts, such as circDscam, circHomer and circStau2, suggesting a function that is independent of the host gene mRNA[58 59]. Predominantly, circRNAs localise in the soma but some can also reach the dendrites and the axon, and others are enriched at the synaptic level[58 78]. Interestingly, the fact that some circRNAs can localise in neurites could be related to a particular cellular condition, suggesting an active transport of these molecules from the cell body to synapses, where they could carry out a specific role. The presence of circRNAs at the synaptic level opens fascinating possibilities about the functional implications. One hypothesis is the potential packaging into vesicles and inside these

structures they could be secreted as messaging or trafficking molecules. Indeed, Lasda and Parker[79] found out that circHIPK3, circZKSCAN1, circASXL1 and circKIAA0182 are secreted in extracellular vesicles, including exosomes and microvesicles. They proposed that might be a cellular clearance mechanism for such stable molecules although another possibility, especially for neuronal cells, is their involvement in signalling pathways between cells. Another hypothesis is their engagement in the transport machinery along neurites; they can serve as carriers or scaffolds to promote cargo delivery to the synapse. Moreover, circRNAs can function in translational regulation at the synaptic level, in specific conditions such as stimuli or stress. One example of a circRNA involved in miRNA stabilisation/transport of other molecules is CDR1as. As mentioned above, it contains 77 binding sites for miR-7 and others for miR-671. Piwecka and colleagues demonstrated that in CDR1as-KO mice miR-7 and miR-671 are affected only in brain tissues, and that these two miRNAs are not affected in all other tissues that normally exhibit very low levels of CDR1as RNA. In particular, the down-regulation of miR-7 in neural tissues of KO animals suggests an involvement of CDR1as in miR-7 stabilisation[26].

Moreover, in the same work the authors showed that CDR1as KO mice have a defect in excitatory synaptic transmission of hippocampal neurons, where CDR1as is more expressed. CDR1as KO neurons show increased spontaneous vesicle release that is not related to synapse formation or vesicle priming activity as they have normal calcium-evoked excitatory postsynaptic currents (EPSCs) but is probably due to an impairment of synaptic response in the KO neurons. In addition, a pre-pulse inhibition (PPI) test, a neurological phenomenon that suppresses the organism's reaction to a stimulus after a weaker peristimulus, revealed a strong difference among WT and KO mice. Altered pre-pulse inhibition can be detected measuring the reaction mentioned above called the startle response, that is altered in neurological disease such as Schizophrenia or other neuropsychiatric disorders and Alzheimer disease[80]. The connection between CDR1as and other neurological diseases as well as Alzheimer's or Parkinson's was previously demonstrated, and this link is once again related to the alteration of miR-7 expression and function. For instance, the down-regulation of CDR1as determines

an increase in mir-7-mediated down-regulation of the ubiquitin protein ligase A (UBE2A), responsible for the clearance of AD-amyloid peptides, thus contributing to their accumulation and aggregation in the cytoplasm of hippocampal neurons[81]. The miR-7-CDR1as axis could also be important for Parkinson Disease, since α-synuclein is a miR-7 target [82]. Nonetheless, a general alteration of circRNAs in Schizophrenia post-mortem biopsies was recently showed by Mahmoudi and co-workers, that speculate about the possible alteration of miRNA availability due to the alteration of a large circRNA/miRNA/mRNA network[83].

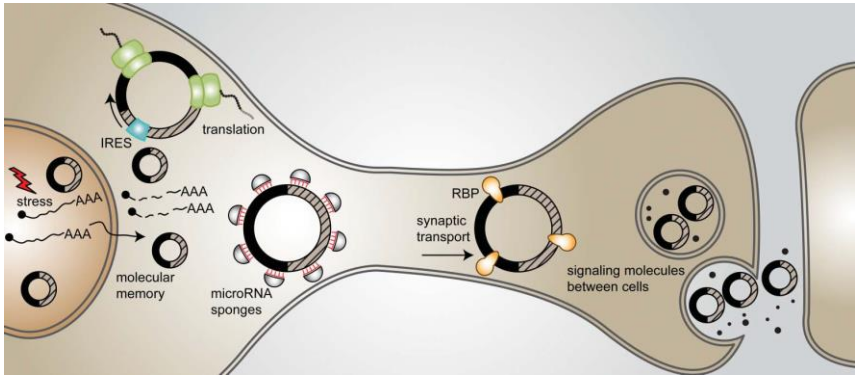

Figure 2: circRNAs role in neuronal system: CircRNAs may be transcribed upon stress and serve as "memory" molecules, as they are extremely stable. CircRNAs can serve as templates for translation into proteins, in the cytoplasm or in synapses. CircRNAs can act as miRNA sponges or active transporters to the synapse or dendrites. CircRNAs may encode information that can be stored or even passed on between cells through microvescicles". (Adapted from Hanan, Soreq and Kadener, 2017)[84].

The high conservation rate of circRNAs (of at least one out of the two specific splice-sites that generate the circRNA)[58] among different species (such as rat, human, mice)[58] [59] [51] and the evolutionary conservation of the expression during development, makes them even more interesting. CircRNA expression undergoes a spatial-temporal regulation during cell differentiation, and brain development. Many studies show the high levels of circRNA expression in the brains of flies, mice, pigs and humans[60] [61] [59] [85].

As mentioned above, You and colleagues showed that circRNAs are expressed at high levels, concomitantly with synapse formation (P10)[59]. In agreement with this observation, Venø and colleagues showed an increase of circRNA expression at day 60 of embryonic development (E60) of pigs, which corresponds to a period of development with high levels of neurogenesis [85]. In flies, circRNAs were found to accumulate with age in the head [61]. Coherently, peaks of circRNA expression have been observe also *in vitro* during P19, SH-SY-5Y neuronal differentiation[58] and in motoneurons (MNs) derived from mouse embryonic stem cells [56].
This last work was carried out in our laboratory; Errichelli and co-workers showed a differential expression of circRNAs in differentiated MNs when compared to mouse embryonic stem cells. Moreover, in the same work many circRNAs have been shown to be altered in FUS/TLS (Fused in sarcoma/translocated in liposarcoma) KO conditions. FUS/TLS is a protein involved in DNA repair, RNA transcription, splicing, import and export[86], and it is also one of the most studied proteins involved in ALS (Amyotrophic lateral sclerosis). The alteration of circRNAs in FUS KO condition prompted us to study the involvement of these molecules in the ALS pathology linked to FUS mutations.

1.6 Amyotrophic lateral sclerosis

ALS, also known as Lou Gehrig's disease, is a MN disease characterised by the progressive degeneration of upper corticospinal, corticobulbar and lower motor neurons[87] [88]. The onset of the pathology usually occurs in mid-adulthood, around 55 years of age, with the exception for juvenile forms of ALS that are characterised by an onset before 25 years of age[89]. Upper MN degeneration determines muscle atrophy with long-standing lesions, while the damage to lower MNs causes decreased reflexes and muscle atrophy due to denervation and dismantlement of motor units. ALS onset can be characterized by the initial degeneration of a specific subtype of MNs. 25% of ALS cases have bulbar onset, and the typical symptoms are difficulty in swallowing and speech. The vast majority of ALS cases have spinal onset, showing general arms weakness. The general loss of the motor unit leads to progressive muscle atrophy and paralysis, rapidly followed by death from respiratory muscle insufficiency that generally occurs within 3–5 years after diagnosis, although some forms of the disease demonstrate protracted survival[87] [88] [90].

ALS is a complex multifactorial disease, classified in familial ALS (fALS) or sporadic ALS (sALS). The causes of sALS are still not fully uncovered: environmental risk factors, sometimes associated with potential genetic predisposition, have been thought to be involved in the pathogenesis of sporadic ALS. A wide range of genes with different mutations have been linked to fALS and the mutations are mainly dominant[91]. The first mutation linked to ALS was discovered in 1993 and resides within the SOD1 gene[92]. SOD1 encodes for the superoxide dismutase protein involved in the conversion of highly reactive superoxide (most frequently produced by errors in mitochondria) to hydrogen peroxide or oxygen; alteration of SOD1 activity causes free radical toxicity. Since then, many other genes have been found to be altered in ALS, and they code for proteins that participate in other different cellular processes, such as protein homeostasis, maintenance of the cytoskeletal structure, glutamate uptake, oxidative stress in microglia, vesicular transport, angiogenesis and RNA metabolism (Fig.4)[87] [93] [94].

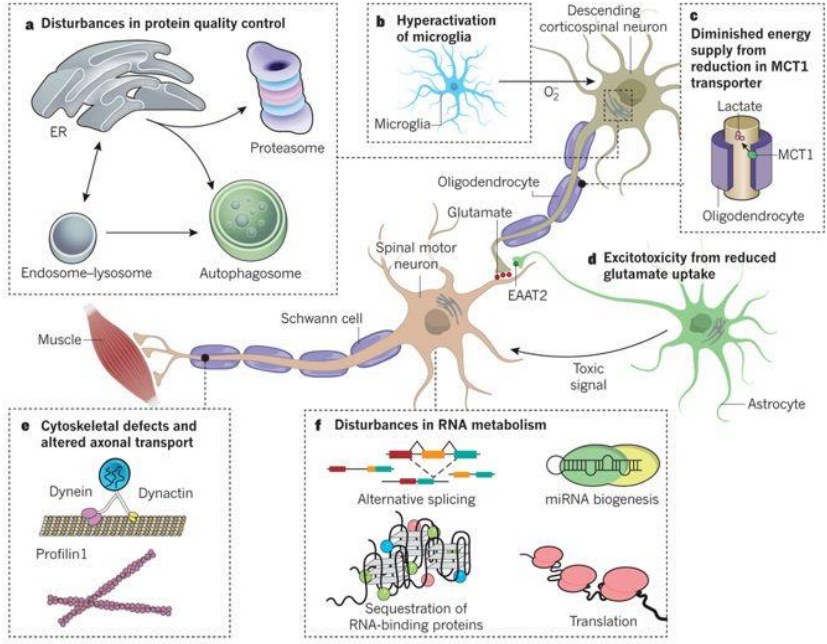

Figure 4: Cell processes altered in ALS: excitotoxicity; microglial defects; cytoskeletal impairment, alterations of protein homeostasis due to perturbation of quality control and the functional and structural alteration of RNA binding proteins (Taylor, Brown and Cleveland, 2016)[87].

In this latter category, a high number of RBPs are involved and in many ALS cases the hexanucleotide GGGGCC expansion in intron 1 of chromosome 9 open reading frame 72 (C9orf72) determines a gain of toxicity through the accumulation of RNA foci in the nucleus[94]. Examples of RBPs genes involved in ALS are Matrin3, Ewing sarcoma breakpoint region 1 (EWSR1), TATA-Box Binding Protein Associated Factor 15 (TAF15)[87] ,heterogeneous nuclear ribonucleoprotein A1 (hnRNPA1, hnRNPA2B1)[95], ATXN2; and TIA1[96], and two of the main studied proteins are TAR DNA-binding protein 43 (TDP-43), and FUS/TLS[86]. All these RBPs have different domains in common: an RNA-recognition motif (RRM), a nuclear localization signal (NLS), and a low complexity domain that is involved in liquid phase separation[96]. The low complexity domain behaves as a prion-like domain and can promote aggregation. FUS

and TDP-43 are usually linked when referring to ALS since they have a similar structure and similar function. They are both involved in the biogenesis of different classes of RNAs, mRNA, lncRNA and miRNA, in canonical and alternative splicing, transport, translation and stability. Both are affected in fALS and in some cases of sALS, and mutations in their prion-like domain or in their NLS can induce their aggregation. Although FUS and TDP-43 are altered only in 5% of fALS cases (Fig.5), it is interesting to notice that the mutation of these proteins is reported in other pathologies related to ALS, such as frontotemporal lobar degeneration (FTLD), characterised by the presence of ubiquitin-positive inclusions. Despite TDP-43 and FUS normally being located in the nucleus, pathological TDP-43 and FUS inclusions are mostly found in the cytosol[97].

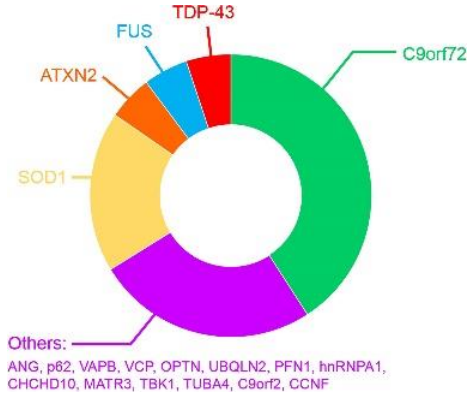

Figure5: ALS related proteins: FUS function and pathological involvement in ALS (Adapted from Ragagnin et al., 2019). FUS is involved in 5% of familial ALS[98].

1.7 FUS protein functions and pathological involvement in ALS

FUS/TLS is a member of the TET protein family that also includes the EWS protein, the TATA-binding protein (TBP)-associated factor. FUS mRNA contains 15 exons coding for a protein of 526 amino acids; this latter contains an N-terminal QGSY-rich region, known to be the prion-like domain with a low complexity structure that confers FUS/TLS the tendency to aggregate, a highly conserved RRM, multiple RGG repeats, a C-terminal zinc finger motif and a nuclear

NLS (Fig.7). The sequence specificity of FUS/TLS binding to RNA or DNA has not been well established yet, however, a common GGUG motif has been identified as a preferential binding site[97 99].

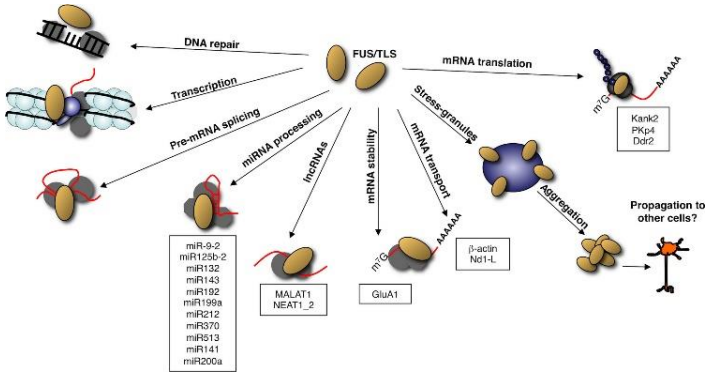

Figure 6: FUS/TLS functions [100] *(Ratti and Buratti., 2016)*

In the nucleus, FUS is involved in many different processes, DNA repair, [101 102], miRNA processing[103], splicing, alternative splicing [104]and in transcriptional regulation [105] (Fig.6). Despite being mainly localised in the nucleus, FUS carries out important roles also in the cytoplasmic compartment and neurites. Numerous works have demonstrated the presence of FUS in dendrites and at the synaptic level of hippocampal neurons, [106 107] its involvement in the transport of RNA-granules[108] and in mRNA translation [109]and stability[110]. Nonetheless, with the high-resolution imaging FUS was found at the post-synaptic level in the early stage of synapse maturation of iPSC-derived MNs, and at the pre-synaptic level at the mature stage[111]. Very recently, Bosco and colleagues showed that FUS is required for Gria2 mRNA processing in dendrites, in order to contrast the high calcium entrance under glutamate excitotoxic stress[112]. Moreover, the Dupuis laboratory demonstrated that FUS is important not only for the neuronal cells but also for the maintenance of NMJ (neuromuscular junction) at the muscular level, regulating the synapse-specific expression of the Acetylcholine receptor[113]. This last finding supports the "Dying back" paradigm, which asserts that the degeneration of MNs in ALS starts from the NMJ, involving the muscle and the synapses[114]. ALS patients with mutant FUS exhibit

a particularly severe disease progression, with 60% of cases having onset of the pathology before 40 years of age. FUS mutations mainly occur in the NLS domain, such as P525L and R521C, inducing FUS cytoplasmic delocalisation [115].

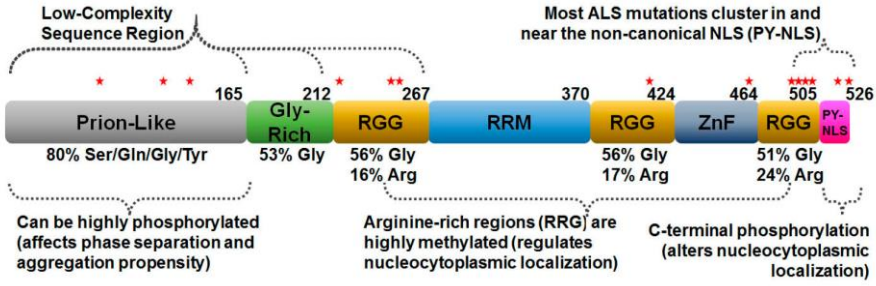

Figure7: FUS /TLS has a low-complexity region that includes all the first part of the protein (N-terminal) and consists mostly of a few different amino acids (80% serine/glycine/tyrosine). The prion-like domain shares sequence composition with domains in yeast proteins that form self-replicating amyloid structures and is highly phosphorylated following certain stresses. The RGG domains contain the triplet repeat motif of arginine–glycine–glycine, which are extensively methylated. The RRM serves to recognise RNA and the zinc-finger domain (ZnF) allows DNA binding. Lastly, the proline–tyrosine nuclear localisation signal (PY–NLS) is among the most affected regions of ALS related FUS mutations. [116]

In particular FUS P525L causes the most aggressive form of ALS with the earlier onset; development of the pathology occurs at 24-28 years of age[117] [115] [97] [118]. To date, it is still unclear whether the pathology is due to the Loss of function (LOF) of FUS in the nucleus or to its Gain of function (GOF) in the cytoplasm, related to its propensity to aggregate; both hypotheses are supported by several findings. LOF of FUS in the nucleus affects all processes that FUS is involved in, such as miRNA and circRNA biogenesis[119] [120] [121] [56]; DNA damage repair, since DNA damage was indeed detected in the post mortem brain of ALS patients [122]; alteration of interactions with transcription factors such as with the transcriptional coactivator PGC1alpha, a master regulator of mitochondrial function

that coordinates gene expression of genes involved in the mitochondrial ROS response[123][124]. Moreover, FUS delocalisation can cause splicing impairment possibly due to mis-localization of splicing factors interacting with FUS[125]; and impairment of nuclear import[115].

FUS GOF is undoubtedly associated to its aberrant massive presence in the cytoplasmic compartment. Gain of toxic function of FUS has been associated to its ability to activate p38 MAPK that compromises the fast anterograde transport mediated by KIN1[126] and has been shown also in Knock-in mice, where the mutant protein triggers autonomous MN loss, that does not occur in KO mice[127].

FUS, together with TDP-43 and other RBPs with low complexity domains, can aggregate in the cytoplasm of ALS and FTLD patients, and co-localise with stress granule (SG) proteins[115] [97]. SGs are cytoplasmic membrane-less particles that assemble upon different stress conditions and require eIF2a phosphorylation[128]. SG formation means a stop in the translational activity of the cells that must contrast the stress. Accordingly, SGs contain different components involved in several RNA-related processes, from the translation machinery, such as translation initiation factors (eIF3, eIF4B, eIF4F), Poly-A Binding Protein 1 (PABP-1), small ribosomal subunits[128] [129], to translational silencing proteins such as T-Cell-Restricted Intracellular Antigen-1 (TIA1 Cytotoxic Granule-Associated RNA-Binding Protein or TIA-1) and TIA1 Cytotoxic Granule-Associated RNA-Binding Protein-Like 1 (TIAR)[130] [131], Cytoplasmic Polyadenylation Element-Binding Protein (CPEB) and Ataxin-2, also altered in ALS.[132] In SGs there are also proteins involved in RNA decay, such as Tristetraprolin (TTP), Z-DNA Binding Protein1 (ZBP1), Argonaut proteins[133] [134] and RNA-binding proteins not related to RNA translation or decay, for example GTPase Activating Protein (SH3 Domain) Binding Protein (G3BP). Moreover, it has been shown that SGs are largely composed by long RNA molecules predominantly polyadenylated, coherent with the presence of RBPs involved in the mechanism of translation [135] [136]. Parker and colleagues showed that RNA-RNA interactions could also be involved in one of the first steps of SG aggregation[137]. Similarly to SGs and in an extremely regulated balance with them, the processing

bodies (P-bodies, PB) are membrane-less cytoplasmic organelles containing mRNAs associated with translational repressors, and the mRNA decay machinery such as DCP1a and 2 (DCP2) [128 138 139]. P-bodies are compact, dense structures visible even in physiological conditions, although their assembly can also be induced in response to stress, indeed they share a large number of proteins including eIF4E, Fas-Activated Serine/Threonine Phosphoprotein (FAST) and 5'-3' Exoribonuclease 1 (XRN1) [128] with SGs. SGs form from mRNAs stalled in translation initiation and can overlap, in some cases, with PBs where mRNAs can undergo decapping and degradation[128]. During RNP granule disassembly, the mRNPs components of P-bodies and SGs can return to translation or be targeted for autophagy, a system for stress granule clearance[140]. Ubiquitin-positive aggregates of mutated FUS and TDP-43 have been found in SGs but not in P-bodies, in ALS and FTLD patients and in cellular model systems[115 127]. The prion-like domain (or low complexity domain) at the N-terminal of FUS allows the liquid phase separation[141], causing protein self-aggregation. This can explain those cases where FUS aggregates but does not colocalise with SGs[127 142 143]. However, FUS aggregation and association with stress granules is strongly dependent on its cellular concentration[144]. Accordingly, the endogenously-expressed WT FUS, mainly nuclear, is generally not found in stress granules in response to these stressors, although some reports have described this observation in overexpression conditions, when the amount of FUS WT increases also in the cytoplasm[145 146]. Nonetheless, in pathological condition, the presence of mutated FUS into the cytoplasm alone is not sufficient to induce the aggregation (Fig.8). The 'multiple-hit model' asserts that a second hit, fundamentally cellular stress such as heat shock or oxidative stress or endoplasmic reticulum (ER) stress, is necessary to lead FUS accumulation in aggregates[97]. Moreover, it has been shown that FUS aggregates can be separated form SGs and the propensity to aggregate, is not only due to the low complexity domain, but also to the presence of an RRM domain and to the bound RNA molecules[147 144]. At the same time, the RNA binding domain allows the recruitment of FUS aggregates to SGs, a "strategy" that seems to provide protection from pathological aggregation that FUS,

with disrupted RNA binding sites, might show[147]. Thus, the aggregation model involved with the pathological condition requires FUS mutated self-aggregation and engagement of RBP components of stress granules; subsequently, due to persistent stress, the aggregates can turn into insoluble fibrillar inclusions causing the fibrillar protein pathology in the disease[144].

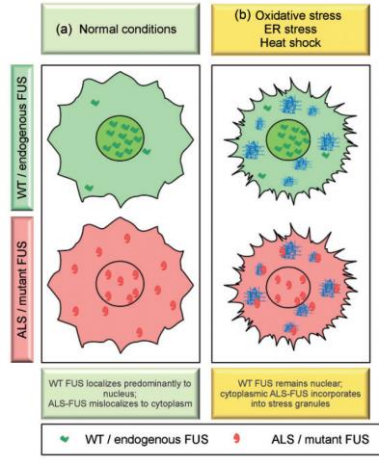

Figure 8: in WT cells upon stress condition FUS remains nuclear, while in FUS-mutant cells the stress induces cytosolic FUS to aggregate with SGs. (Adapted from Sama, Ward and Bosco., 2014)[148].

The ALS-related mutants, FUS P525L and R495X, exhibit the most robust levels of both cytoplasmic delocalization and stress granule colocalization[115]. FUS-mediated recruitment and incorporation into stress granules, marked with TIAR and G3BP is a reversible process [149] [150], however, it has been suggested that the accumulation of FUS proteins within SGs might be a disease-initiating event and that a subsequent chronic stress eventually leads to the irreversible pathological aggregation of these proteins. Indeed, aggregates of FUS, marked with SG proteins are found in ALS patients[115].

2. AIM

It has been recently demonstrated by our lab that the FUS protein is involved in the biogenesis of circular RNAs (circRNAs) in murine motoneurons (MNs)[56]. Among the most expressed and affected by FUS depletion we selected circ-16 and circ-31, the first arising from exon 2 of the Dlc1 gene and the second from exons 2-3-4-5 of the Hdgfrp3 gene. These two circRNAs are conserved between mouse and human and upregulated during MN differentiation in both model systems. Notably, while circ-16 is specifically expressed in MNs, circ-31 results to be expressed also in other neuronal cell types. The main aim of this study is to investigate the function of circ-16 and circ-31 in MNs and their potential involvement in ALS. For this purpose, we generated MNs from murine embryonic stem cells (mESCs) carrying the P517L FUS mutation, which causes a relevant FUS delocalization in the cytoplasm and is linked to one of the most severe forms of familial ALS. In these cells, we set up and performed *in situ hybridization* studies to investigate whether the presence of mutant FUS could affect circRNA subcellular localization. We also mimic the formation of cytoplasmic aggregates that occur in ALS by applying an oxidative stress to wild type and mutant MNs, in order to check whether also circ-31 and circ-16, as other cellular RNAs, could be trapped in these membrane-less compartments and whether this phenomenon is dependent on the presence of mutant FUS.
In parallel, we also performed circRNA pulldown experiments in order to identify RNA and protein interactors and set up a CRISPR/Cas9-based strategy to knock out circRNAs while maintaining the expression of the corresponding host genes unaltered.

3. RESULTS

3.1 CircRNA identification

Previous work performed by Errichelli and colleagues, which included a high throughput approach (Ribo(-)RNA-Seq), found that the expression of several circRNAs expressed in murine motoneurons was affected by FUS depletion[56]. Among them, we decided to focus our attention on two of the most expressed circRNAs in motoneurons: circ-31 and circ-16, arising from exons 2-3-4-5 of Hdgfrp3 (Hepatoma-Derived Growth Factor-Related Protein 3) mRNA and exon 2 of Dlc1 (Deleted In Liver Cancer 1) pre-mRNA (isoform 1) respectively. These two selected circRNAs show an opposite behaviour in FUS KO MNs with respect to WT condition. In particular, circ-31 is down regulated while circ-16 is up-regulated. Moreover, the linear isoform of circ-31 is not affected in FUS KO conditions while the Dlc1 linear isoform is down-regulated, thus showing an opposite trend with respect to circ-16. RNA-Seq analysis was also performed in P517L FUS mutant MNs and in this condition, only the expression of circ-16 varied and resulted to be upregulated, as observed in FUS-KO conditions (Table 1).

	WT CPM circular	WT CPM linear	FUS-KO CPM circular	FUS-KO CPM linear	FUS-P517L CPM circular	FUS-P517L CPM linear
Hdgfrp3 (circ-31)	67	234	40	239	68	198
Dlc1 (circ-16)	43	280	65	294	70	248

Table1: Normalized reads obtained from the RNA sequencing of circ-31 and circ-16 and their corresponding linear counterparts in a pure population of WT, FUS KO and FUS mutant MNs.

CircRNA expression was assessed in MNs derived from the differentiation of mESC carrying a GFP reporter gene under the MN-

specific Hb9 promoter. After six days of differentiation, embryoid bodies (EBs) that contain a neuronal population, and in particular MNs are dissociated. Single cells can then be sorted for GFP expression in order to obtain a pure population of MNs only. Through RNA-Seq analysis and Realtime PCR, we have observed a strong increase of circ-16 expression in the pure population of MNs, while its expression is almost absent in the GFP- cells and in mESCs. On the other hand, circ-31 resulted expressed also in GFP- cells that contain neuronal cells such as interneurons, astrocytes and glia but not MNs (Fig.9).

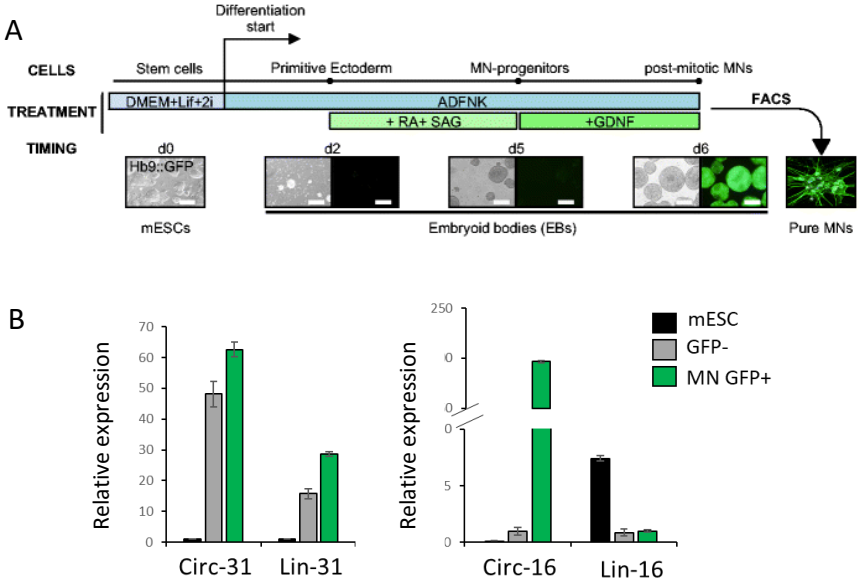

Figure 9: A) mESC differentiation into MNs using retinoic acid and activating the sonic hedgehog pathway (adapted from Capauto et al., 2018.) B) Differential expression of circ-31 and circ-16 with their corresponding linear isoforms in mESCs, GFP- and GFP+ populations.

CircBase (http://www.circbase.org/), a database containing the annotation of different circRNAs expressed in mouse and human tissues available online, allowed us to determine the expression of our circRNAs in these tissues (Fig.10). Circ-31 was found to be expressed in different mouse tissues and in several brain regions specifically, such as cerebellum, mid brain and forebrain. It is also

expressed in the diencephalon, cerebellum, occipital lobe, frontal cortex, parietal and temporal lobes. Differently, circ-16 was expressed only in the temporal lobe in human samples, while in mouse tissues, and was found in the brain, head, cerebellum, frontal cortex and hippocampus. Therefore, both the circRNAs are enriched in neuronal cell types.

Circ-31

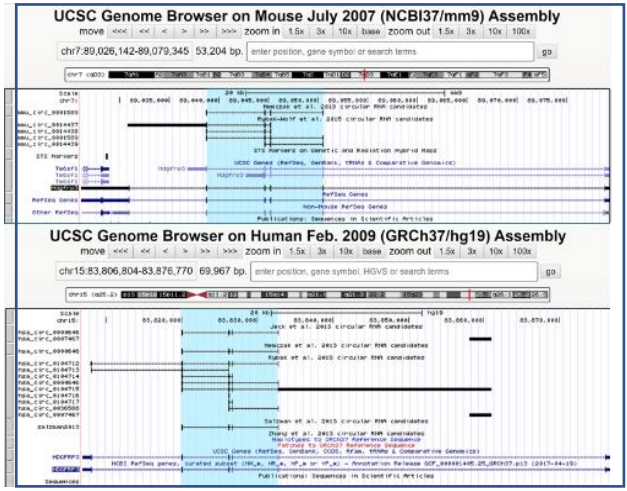

Circ-16

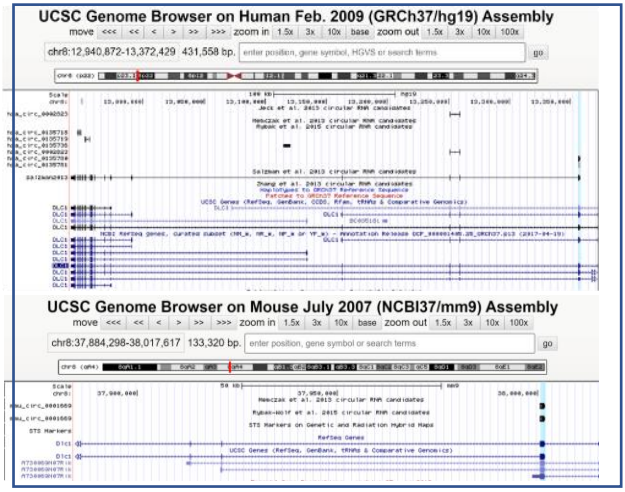

Figure 10: circBase annotated circRNAs visualized on the UCSC browser. Circ-31 arises from the hdgfrp3 gene and circ-16 from Dlc1.

Since circRNAs are enriched in the neuronal system and most of them are also localized at synapses, we decided to look at published RNA-Seq data produced by Ryback-Wolf and co-workers[58] using RNA extracted from the mouse whole brain and synaptosomes. We found that both circ-16 and circ-31 where enriched in the mouse whole brain, coherently with circBase data, and that circ-31 was also enriched in synaptosomes. Therefore, we decided to analyse the localization of circ-16 and circ-31 in mESC-derived MNs by *in situ hybridization (ISH)*. We differentiated mESCs in MNs following a well-established protocol[151]. After six days of differentiation we obtained embryoid bodies (EBs) that were then dissociated and plated as a mixed population of neuronal and MN cells on poly-ornithine/Laminin-coated glasses. 36 hours later we fixed the cells with 4% PFA in order to perform ISH. We set up the ISH on our *in vitro* differentiated MNs by using the Basescope™ approach. This technology provides two Z-like probes that can specifically target the 3' and 5' ends of the backsplicing junction, therefore, only when the two Z-like probes are close to each other (this occurs only on circRNA molecules and not on the linear ones) they are recognised by another longer L-shaped probe. This latter is subsequently bound to a large set of smaller probes allowing the amplification of the signal. The same approach can be applied to linear transcripts with the two Z-like probes targeting the canonical splice junction (Fig.11a).

A

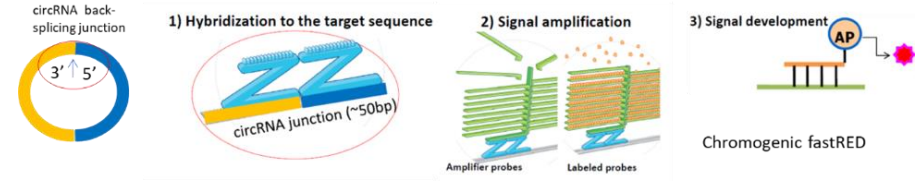

B

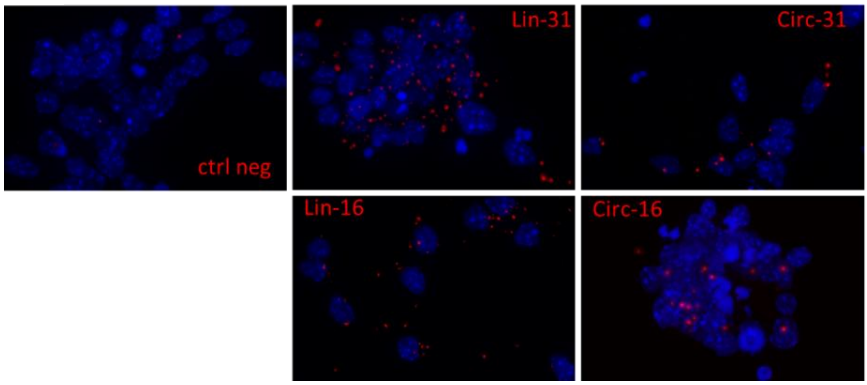

Figure 11: A) Basescope™ technology illustration. Two Z-probes can be recognised by another long L-like shaped probe only when these two are close together. This strategy allows the specific targeting of the backsplicing junction, avoiding non-specific signals due to the linear isoform B) ISH for the negative control (ctrl neg), lin-31, circ-31, lin-16 and circ-16. Targets are in red and the nuclei in blue.

We tested the efficiency of the technique to visualise both linear and circular molecules, and we also used negative control probes, targeting a bacterial RNA not present in our cellular system. The negative control allows us to exclude that the detected signals were not-specific and due to the pairing of the probes to non-specific targets. For the linear staining we used probes targeting a region not included in the circRNAs and we observed that the number of dots corresponding to the linear molecules was higher than the circular ones. This was seen for both circ-31 and circ-16, which was in agreement with results from RNA-seq experiments (Fig. 11b). We also confirmed circRNA expression in several neuronal cells in the mixed population by combining the ISH protocol with an immunofluorescence one. We labelled MNs using an antibody against Islet-1, which is an essential factor involved in the formation of mature and functional[152] MNs, and all neuronal cells by using a

tubulin III antibody (TujI). We observed that, as previously demonstrated, circ-31 is a neuronal circRNA expressed in all tubulin III-positive cells (MNs and other neuronal cells present in the mixed population) while circ-16 resulted to be specifically expressed in MNs, the Islet-1- positive cells (Fig.12).

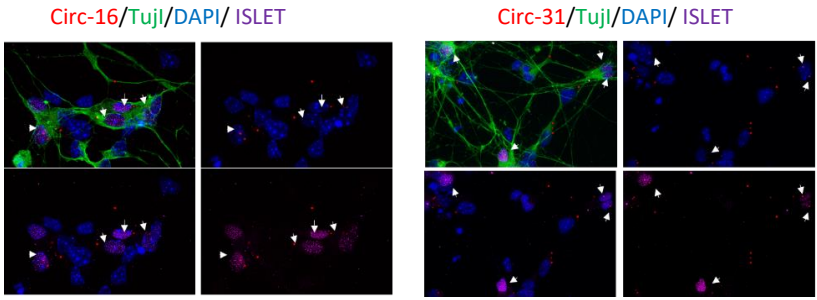

Figure 12: ISH of circ-16 and circ-31 in red, IF of tubulin III in green and islet in purple. Circ-16 localizes only in MNs while the circ-31 signal spreads in MNs and other neuronal cells present within the MN mixed population. White rows indicate islet-positive cells.

We also observed that circ-31 and circ-16 were distributed both in the soma and in the neurites of neuronal cells. In particular, we observed that circ-31 was appeared in the neurites more frequently than circ-16 that instead was also detected in the nucleus (Fig.13b). The study of circRNA sub-cellular localization could help the understanding of the role of these molecules in the neuronal system. For instance, the localization of circ-31 in the soma and in neurites suggests that the molecule might move along the neurites to carry out a function at the synaptic level and eventually move back to the soma. We next decided to keep MNs in culture in order to increase MN maturation. Although MNs are mature cells expressing all the related markers at the end of the differentiation protocol [153], maintaining MNs in a plate with surrounding cells (interneurons, astrocytes, and glia) induces them to elongate neurites and form synapses, interacting with the other neuronal cells. In these cells we performed *ISH* and we focused on circ-31 since circ-16 was mostly detected in the soma and in the nucleus of MNs (Fig.12 and Fig.13a-b). We observed an increasing number of the circ-31 spots during motoneuron

maturation. Indeed, at MN-d3 (day six of differentiation plus three of MN maturation), we observed an increase of circ-31 spots along neurites and this number was even higher at MN-d6 (Fig.13c). These observations agree with the presence of circ-31 in synaptosomes detected by RNA-Seq as described above.

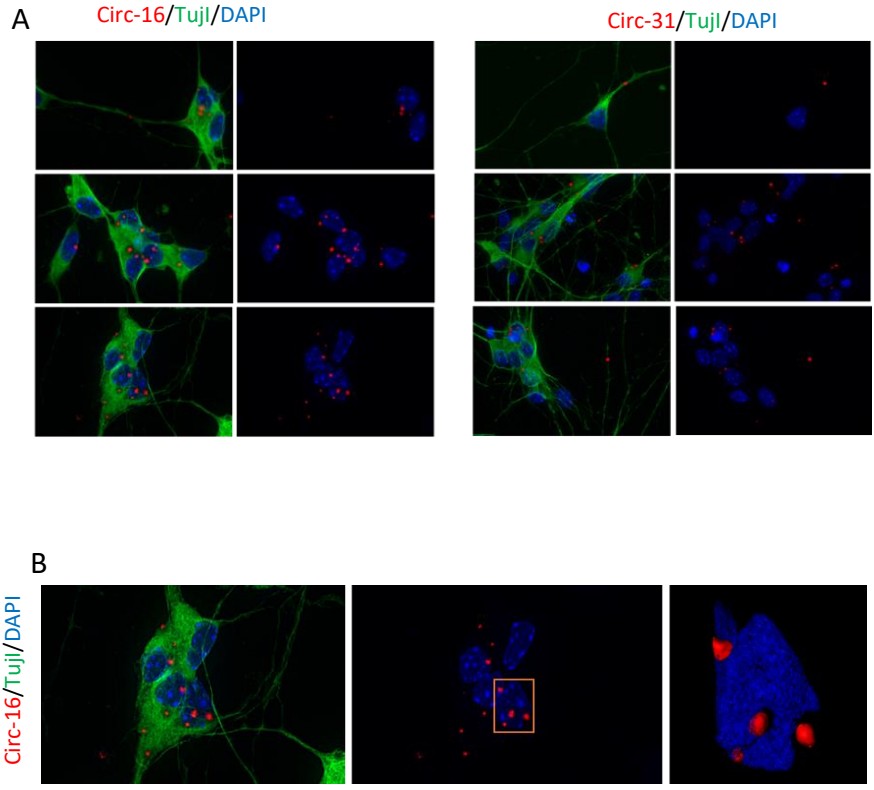

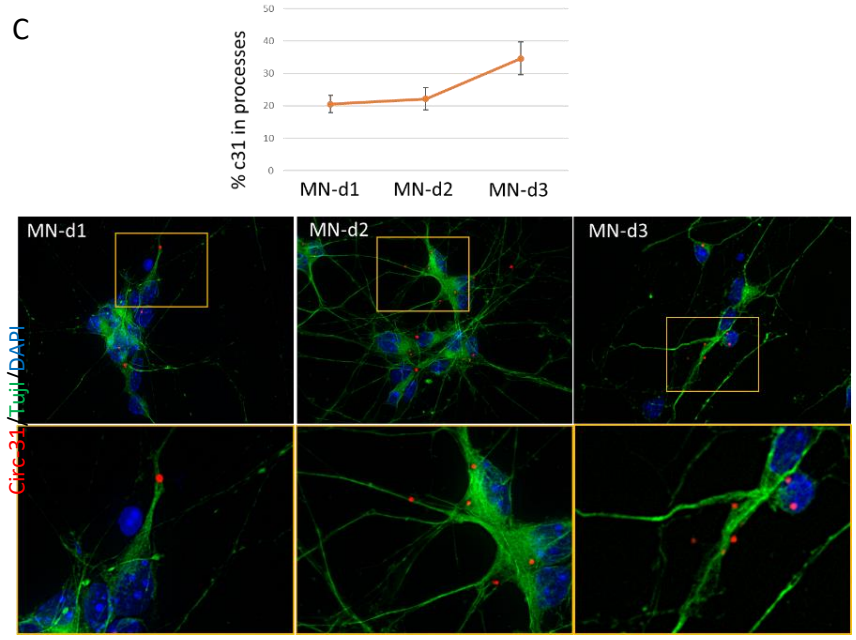

Figure 13: ISH shows that A) circ-16 is mainly localized in the soma and sometimes in the nucleus (B), while circ-31 is in the soma (A) and frequently in the neurites and this increases with motoneuronal maturation (C). Tubulin III in green, circRNAs in red and nuclei in blue.

3.3 CircRNA localization in pathological conditions

As mentioned above, we previously demonstrated that circ-16 and circ-31 are affected in FUS KO MNs. FUS is a DNA/RNA binding protein also involved in canonical and alternative splicing as well as in backsplicing. This protein also plays an important role in neurodegenerative diseases such as ALS and FTD, where different mutations of the protein, in particular in the nuclear localization signal, induce the re-localization of the protein from the nucleus to the cytoplasm. Moreover, in stress conditions, cytoplasmic FUS aggregates form granules that under persistent stress can eventually become insoluble. Furthermore, work from different research groups has shown that in cell cultures and in ALS patient-derived iPSCs differentiated into MNs [149], mutant FUS can aggregate and those aggregates can localise into SGs, upon stress conditions. Since our circRNAs depend on the presence of FUS and despite their expression not being altered in FUS mutant conditions, we asked whether the delocalisation of FUS could affect the localisation of circRNAs and whether FUS aggregation upon stress conditions could have the same or a different effect. Therefore, we used FUS mutated cells (FUS-P525L) and looked at the localization of circRNAs, under normal and stress conditions. We observed that the localization of the two circRNAs understudy was not altered (Fig.14) when comparing WT and FUS mutated cells, firstly in physiological conditions. Indeed, we observed circ-31 in the soma and neurites of neuronal cells; and circ-16 preferentially in the soma and more rarely in the nucleus of MNs. We then applied oxidative stress in order to simulate FUS aggregation by treating the cells with 0.5 mM arsenite for 45 minutes. The incubation of cells with arsenite induces the production of reactive oxygen species (ROS), including free radicals that activate heme-regulated inhibitor kinase (HRI) that phosphorylates eukaryotic translation initiation factor 2α (eIF2α). Phosphorylation of eIF2α prevents the recycling of the ternary tRNAMet-GTP-eIF2 complex resulting in stalled translation initiation complexes and initiates SGs formation [131].

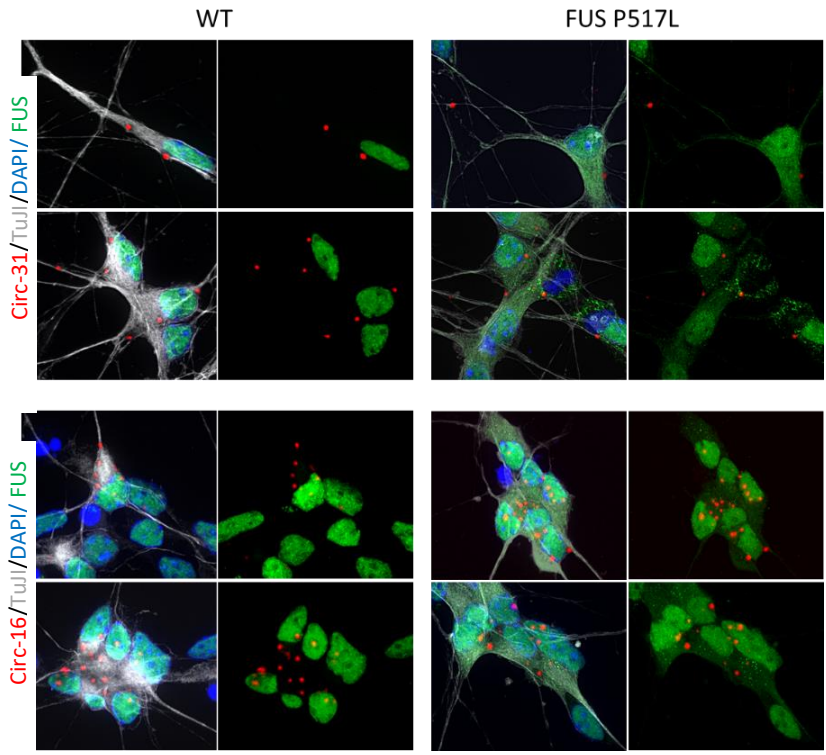

Figure14: ISH and IF for FUS and tubulin in physiological condition. Circ-31 and circ-16 localization is not altered. FUS (green); Tubulin (gray); circRNAs (red); nucleus (blue)

In order to test whether oxidative stress might compromise neurite localization of circRNAs, and whether this phenomenon occurs differently between WT and FUS mutant conditions, we treated WT and FUS mutant cells with arsenite. After 45 minutes of this treatment we observed the formation of SGs and FUS aggregates. By performing IF and *ISH* we checked the integrity of the cytoskeleton, through the tubulin beta III staining (TujI), and the localization of circ-31. We counted circ-31 spots that were localized in neurites and we compared the untreated with the stress conditions. We observed that circ-31 localization was affected upon oxidative stress and that the presence of circ-31 in neurites decreases, both in WT and in FUS mutant conditions (Fig.15). These findings suggest that upon stress,

circ-31 localization is altered due to a putative anterograde transport that occurs in this type of stress condition, or because it is retained and blocked in the soma.

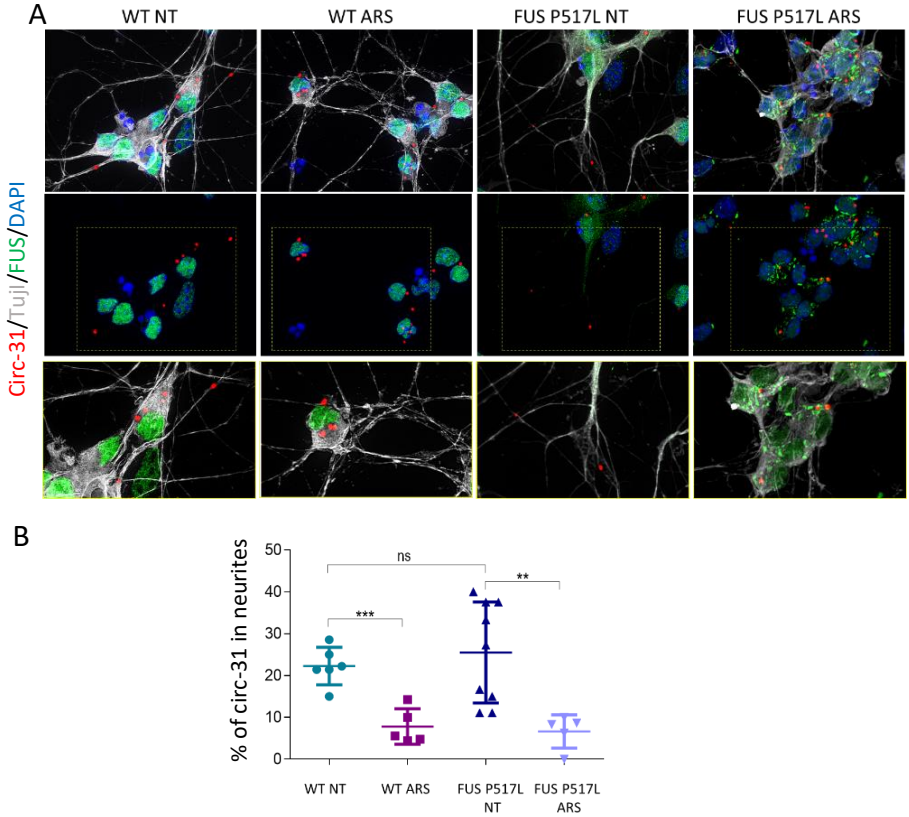

Figure 15: A) WT and FUS mutant cells show no difference in circ-31 localization in a non-treated condition (NT), while both show a retention of circ-31 in the perinuclear region upon oxidative stress performed with 0.5mM arsenite for 45 minutes (ARS). FUS (green); Tubulin (grey); circ-31 (red); nucleus (blue). B) Scatter plot of percentages of circ-31 into neurites, obtained in the different images analysed, with mean and standard deviation. Statistical analysis performed with GraphPad Prism: non-parametric test, Kolmogorov-Smirnov (N≈100 spots for condition).

Moreover, by analysing circ-31 localization in arsenite treated FUS mutant MNs, we noticed that several circ-31 molecules were trapped

into FUS aggregates (Fig.16), suggesting that in these cells the retention of the circRNA upon oxidative stress might be due to, at least in part, its localization into FUS aggregates. In order to gain insight regarding this phenomenon, we firstly used a computational approach, the ComDet plug in of the ImageJ program in order to count the number of circ-31 particles incorporated into FUS aggregates. This approach was combined with a manual one and the two results were then integrated. In particular, the manual approach consists in looking at the single focal plane on the Z-axis of pictures acquired with the confocal microscope, and in considering the circRNA within FUS aggregates only when the two molecules are on the same focal plane. Eventually, we also performed 3D rendering in order to overcome the bias of the 2D Z- stack projection. All these analyses allowed us to determine that more than 30% of circ-31 spots colocalize with FUS mutant granules upon ARS conditions and that this does not occur in normal conditions even though mutant FUS resulted to be delocalised in the cytoplasm (Fig.16b).

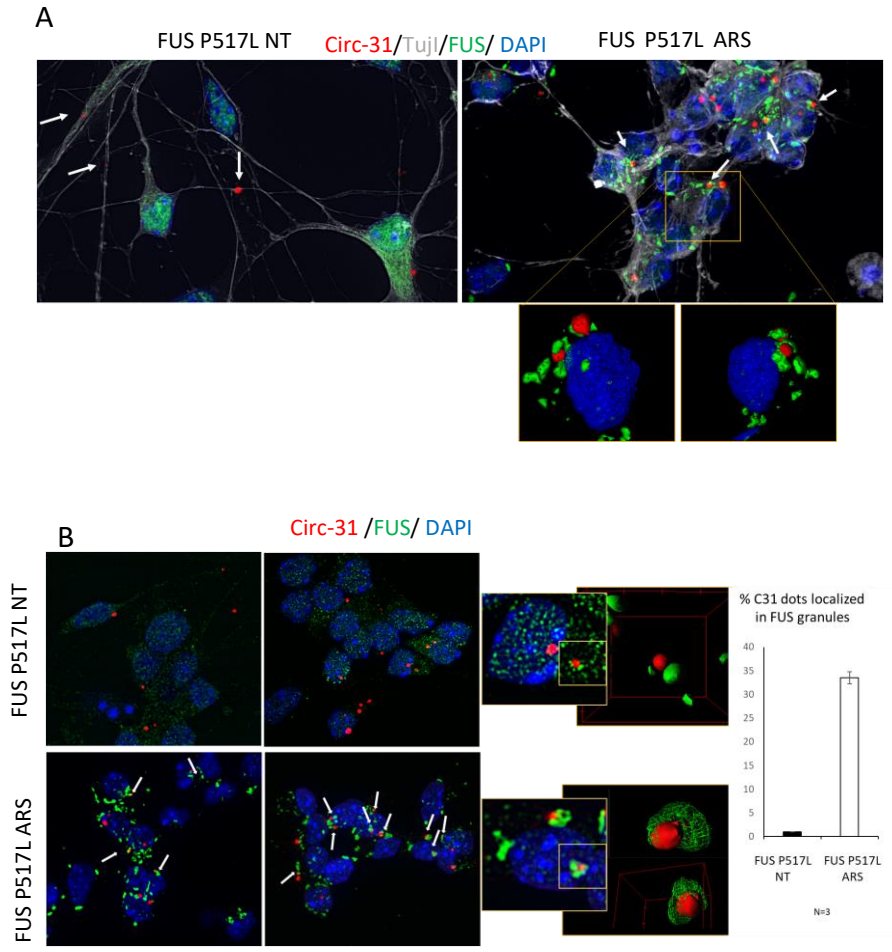

Figure 16: A) Non-Treated (NT) FUS P517L cells show circ-31 in neurites while it is retained in soma and possibly caught into mutant FUS aggregates upon stress. White arrows indicate circ-31 in the neurites of NT cells and into FUS aggregates in ARS-treated cells. B) More than 30% of circ-31 goes into FUS mutant granules upon ARS conditions while no colocalization was detected in NT cells. White arrows indicate circ-31 into FUS aggregates in ARS-treated cells. 3D rendering allows us to verify the overlapping the molecules. FUS green, circ-31 red, nuclei blue. N=3 different biological replicates; ≈100 spot for replicate.

3.3.1 Circ-31 in FUS granules and SGs

Since FUS aggregates very often colocalize with SGs, we decided to see whether circ-31 was differentially retained in FUS-positive SGs versus FUS-only aggregates (both present only in mutant cells). Moreover, since we have observed retention of circ-31 in the perinuclear region also in WT cells treated with arsenite (Fig.15), we decided to investigate whether this behaviour was driven, in WT cells, by retention into SGs. Therefore, we performed IF experiment using antibodies against TIAR, a universal marker for SGs, treating the cells with 0.5 mM ARS for 1h. We used a longer treatment since we wanted to obtain bigger SGs that are more comparable to those reported in literature[149]. Comparing WT and FUS P527L arsenite treated cells, we observed that circ-31 is present also in TIAR positive SGs in WT conditions; however, the number and the distribution of the circRNA spots retained into SGs differed between WT and FUS mutant cells (Fig.17). Indeed, figure 17 shows the results of the colocalization analyses performed: the number of circ-31 dots colocalizing with TIAR positive SGs is higher in FUS mutant than in WT conditions (Fig.17), suggesting that the presence of mutant protein retention favours the retention of circ-31 in SGs. In this case, the quantification was supported by a manual approach by looking at molecules on the same focal plane and occasionally by performing 3D rendering, which is useful for excluding artefacts as described above. Indeed, in the colocalization analyses of circ-31 with SGs in WT conditions, the 3D rendering allowed us to determine that not only the presence of circ-31 in SGs was definitely lower than in the FUS mutant conditions, but also that the circ-31 and TIAR signals were in close proximity rather than completely overlapping.

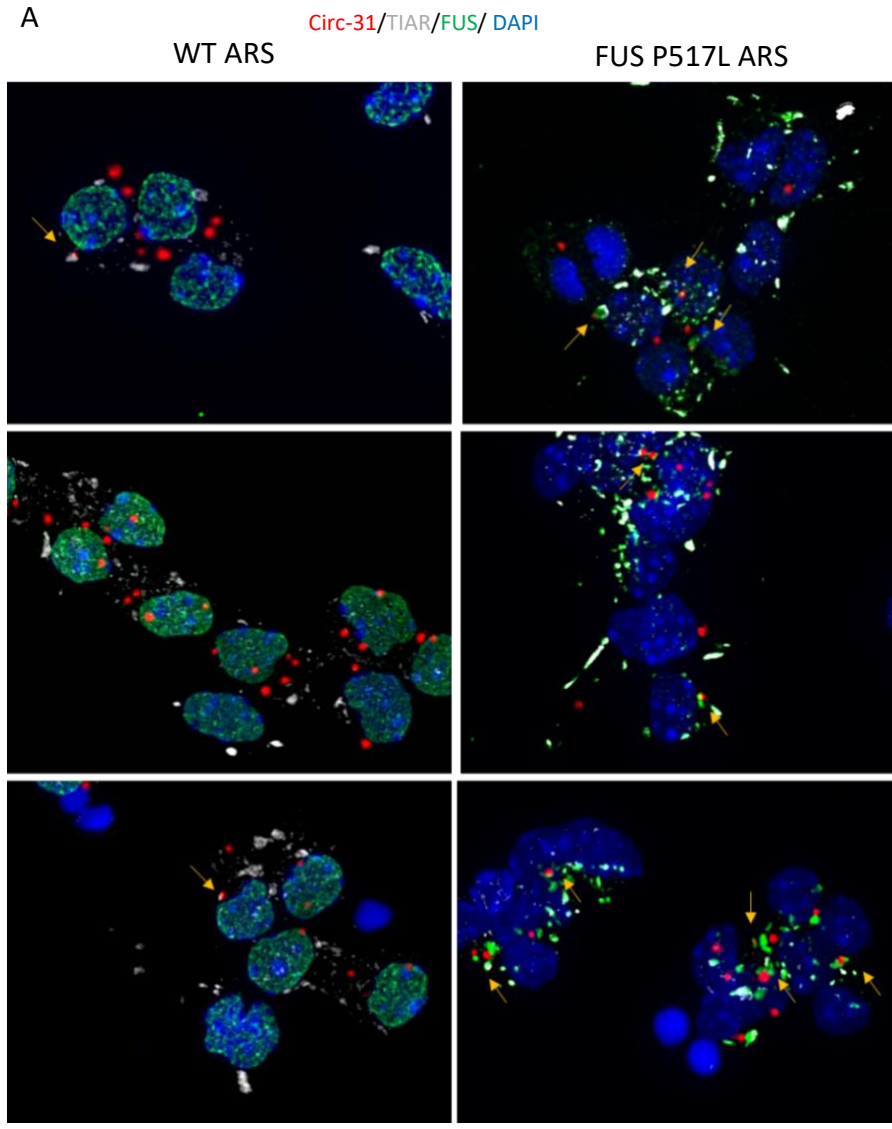
A
Circ-31/TIAR/FUS/ DAPI
WT ARS
FUS P517L ARS

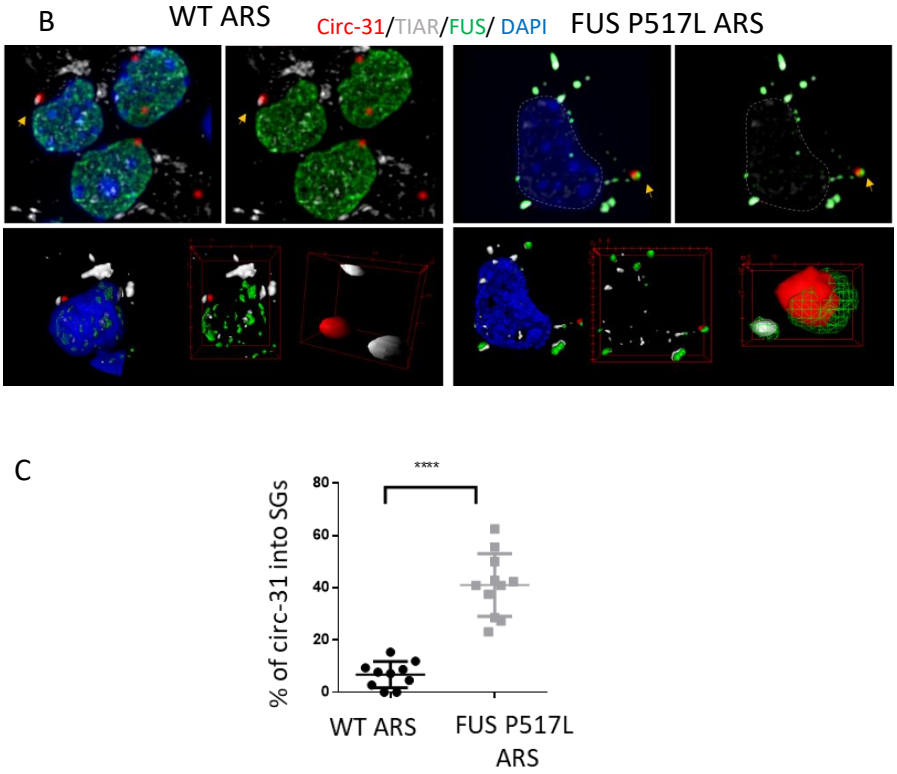

Figure17: FUS (green); Tubulin (grey); circ-31 (red); nucleus (blue). A) WT ARS cells versus FUS mutated cells show different circ-31 retention into SGs. In WT cells the retention of circ-31 in SGs labelled with TIAR, is almost absent, while it is visible in FUS mutated cells. B) In order to avoid counting false colocalizations, we counted molecules on the same focal plane and eventually performed 3D rendering. Molecules not on the same focal plane do not colocalise in the 3D. With this approach we count the number of dots in SGs in WT and FUS P517L conditions, where the localization is strongly major; showed in the scatter plot with mean and Standard deviation. Statistical analysis performed with GraphPad Prism: non-parametric test, Kolmogorov-Smirnov (C). (N≈200 cells for each condition).

In greater detail we noticed that the signal distribution of TIAR and FUS around circ-31 resulted different. In particular, we analysed the peak of intensity of the different molecules and we observed that the peaks for circ-31 and TIAR do not line up, both in WT and FUS P517L conditions (fig.18b). In this latter we looked at granules where both TIAR and FUS were colocalising with circ-31, and even in these cases we noticed the absence of correspondence between the circ-31 and TIAR signals, but not between circ-31 and FUS (Fig.18). This observation together with the propensity of circ-31 to localize in SGs only in FUS mutant cells, again suggests the possibility that the circ-31 localization in SGs is tightly related to the presence of mutant FUS.

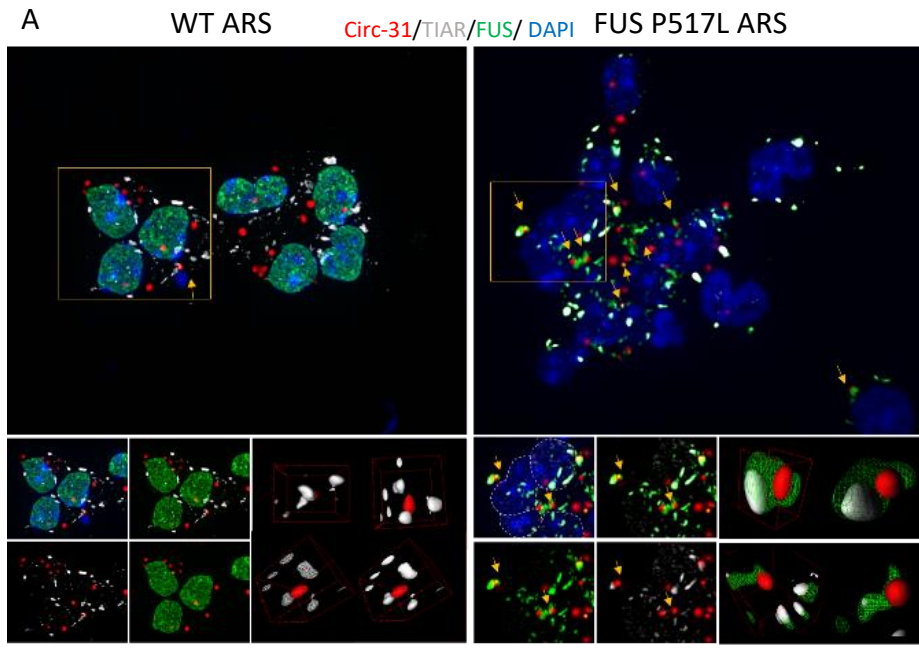

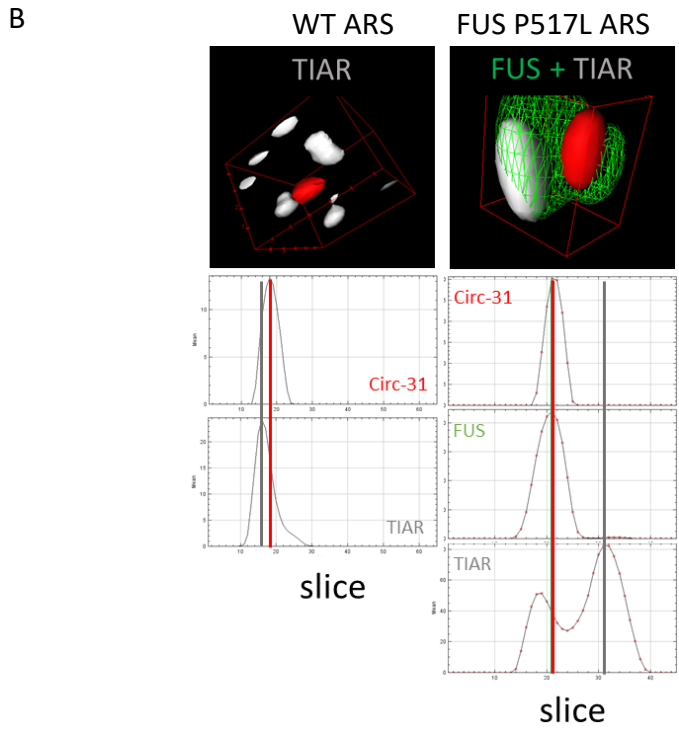

Figure18: (A-B) TIAR (grey) and FUS (green) show a different signal distribution around circ-31 (red). TIAR is mostly close to circ-31 and not overlapping, both in WT and mutated cells, while FUS, in mutated cells, is mostly overlapping with circ-31. Signal distribution is fully overlapping for FUS and circ-31 while it is distant among TIAR and circ-31(B).

Additional topological analysis of the granules was then performed by looking at the 3D disposition of the signal along the x, y, and z axes, only in mutant cells, in order to see whether circ-31 was closer to FUS than to TIAR. The work flow comprises several steps: 1) counting the spots of circ-31 localizing into SGs with FUS or TIAR or with both, using the ComDet plugin, initially without any discrimination among the different granule topologies; 2) correcting the counts via the manual approach as described above and at the same time record all the information regarding the granule structure

and topology; 3) generation of categories concerning the position of TIAR and FUS around circ-31. As a result of these analyses we mainly observed two categories of granules containing circ-31: FUS-only positive granules, where TIAR is not present, and FUS and TIAR-positive granules. This latter was sub classified in:

- granules with FUS and TIAR totally overlapped with circ-31;
- granules with FUS totally overlapped with circ-31 and TIAR in proximity;
- granules with FUS in proximity and TIAR totally overlapped;
- granules with FUS and TIAR both in proximity.

Overlapping and proximity refer to the signal distribution of the molecules. For this classification we supported our manual observation with other two ImageJ plugins: 3D-Object counter, that gave us a mean of distance of the spots that we consider in proximity ($0.66\pm0.2\mu m$) or overlapping ($\leq 0.66\pm0.2\mu m$) with the granules; JaCoP, in order to obtain a Pearson's correlation coefficient, with a range among 1 (fully overlapped, usually a molecule colocalizing with itself) and -1 (no correlation) that tell us how two signals are correlated and potentially overlapped (Fig.19). 60% of circ-31 was found in FUS-positive granules accordingly to ComeDet; however, by using a manual approach we observed a mean of 36% of circ-31 in the granules. Subsequently we observed that among them, around 50% of circ-31 spots were in granules positive only for FUS and not for TIAR (FUS-ONLY) (Fig.19). The remaining spots were colocalizing with both TIAR and FUS, and mainly belonging to the subclasses of granules with both the proteins overlapped, called TIAR/FUS totally overlapped (T/F ov) and to the subclass with FUS overlapping and TIAR in proximity (F ov/Tprox) (Fig.19). To summarise, the presence of mutant FUS seems to be required for the recruitment of circ-31 into SGs while the presence of TIAR seems to be dispensable. Coherently with this, 50% of circ-31 spots are present in FUS-ONLY granules, while the remainder is associated to FUS/TIAR-SGs and no circ-31 was observed in SGs not positive for FUS.

A

FUS P517L ARS: topologic characterization of the granules

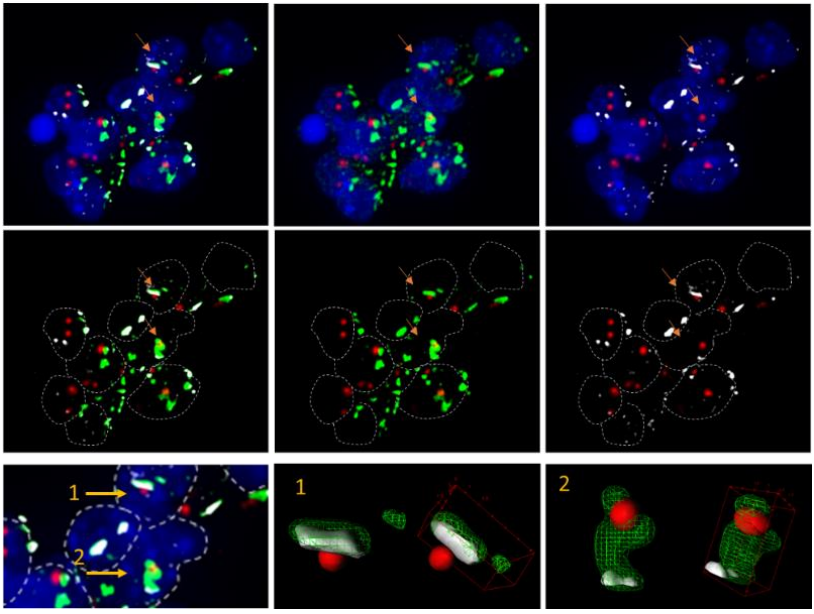

Circ-31/TIAR/FUS/ DAPI

B

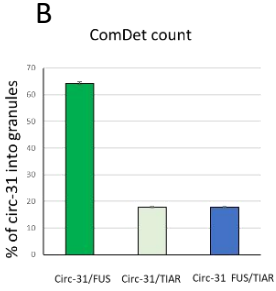

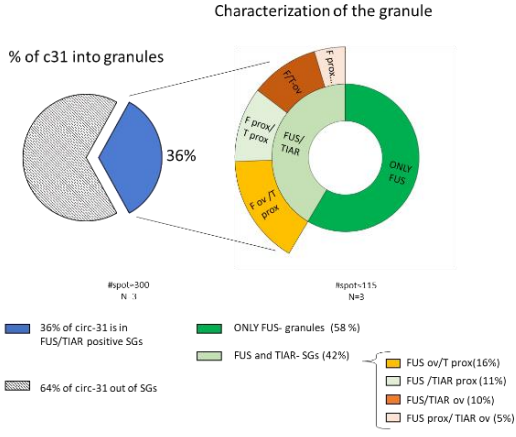

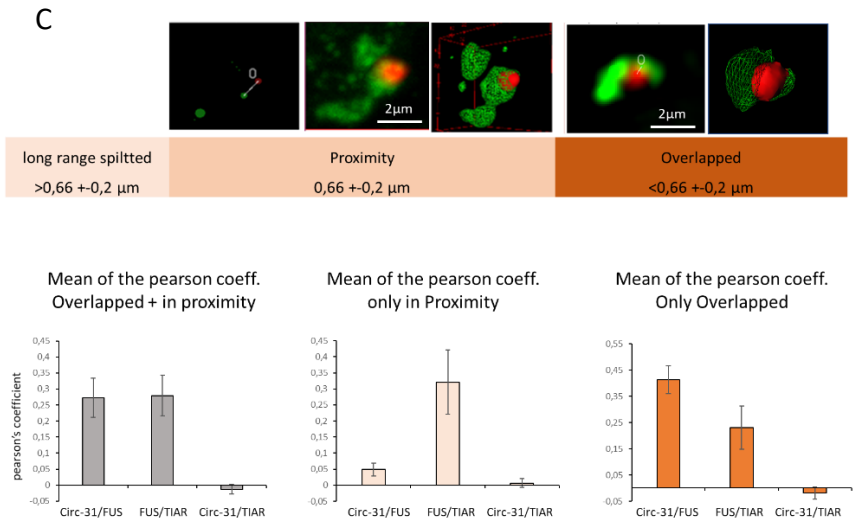

Figure 19: A) Localization of circ-31 in granules of FUS P517L cells, treated with arsenite. Circ-31 overlaps only with FUS or in some cases also with TIAR. The 3D rendering show one example of FUS and TIAR in proximity of circ-31(n°1) and another example of FUS totally overlapped with the circRNA(n°2). B) Subclassification of circ-31/granule topology. We observed that 36% of circ-31 spots are in the granules and half of them are only in FUS-positive granules while the others are in SGs labelled with TIAR. Among them we identified, the granules where FUS is totally overlapped with the circRNA while TIAR is in proximity, as the most enriched class. Legend: FUS ov/ T prox 16% (FUS totally overlapped and TIAR in proximity); FUS / T prox 11% (FUS and TIAR both in proximity); FUS/ T ov 10% (FUS and TIAR totally overlapped); FUS prox /T ov (FUS in proximity and TIAR totally overlapped). N= 3 replicates and #spot= number of spots (N=300 for the count and 115 for the topologic characterisation). C) The Pearson's coefficients for colocalization analysis circ-31 with FUS; FUS with TIAR and circ-31 with TIAR. The first graph represents the mean of Pearson's coefficient obtained for a small cohort of granules where FUS and TIAR where both present. The second graph is the mean of Pearson's coefficient obtained for a cohort of granules where FUS was in proximity and the third where FUS was totally overlapped with circ-31. In all the cases TIAR/circ-31 always have a lower value compared with FUS/circ-31.

Moreover, we observed that FUS signals are mostly overlapped with the circ-31 ones while TIAR is more frequently found in proximity, suggesting that FUS is spatially closer to circ-31 in comparison with TIAR. Then, in order to corroborate the spatial analysis, we extrapolated Pearson's coefficient for a cohort of randomly selected details (of SGs and circ-31 colocalizing). We divided them considering FUS's spatial arrangement, regardless of the TIAR disposition. Therefore, we separated the details in FUS totally overlapped and FUS in proximity and extrapolated a mean of the Pearson's coefficient for these two groups separately. As expected, we observed that Pearson's coefficient of FUS totally overlapped details was higher than those in proximity. While, in both the groups analysed, the Pearson's coefficient among circ-31 and TIAR was always close to zero. This result supports the hypothesis that FUS is in tight proximity to circ-31 and is potentially the first player to catch the circRNA in the cytoplasm, trapping it into SGs or FUS granules. Additionally, we performed all the analyses described above for circ-16. Since this circRNA does not often localize in neurites we directly checked whether it would localize into SGs under stress conditions. We observed that also circ-16 localises into FUS-granules in FUS P517L MNs and sometimes also into SGs in WT conditions (Fig.20). Topological analysis showed that circ-16 is mostly in proximity with FUS and not totally overlapping (Fig.20c-d). Therefore, by counting the granules, TIAR and/or FUS positive where circ-16 was in proximity or totally overlapped, we obtained results similar to the ones for circ-31: 13% of circ-16 spots localise into WT SGs and almost 40% into FUS mutant granules. Nevertheless, considering only the totally overlapped granules, we did not obtain a significant difference between WT and FUS mutant cells, meaning that circ-16 joins SGs with the same efficiency in both conditions (Fig.20c-d). In addition, performing ComDet counts on circ-16 in FUS-positive granules we obtained a result comparable to the count that we obtained, manually, excluding the granules in proximity (Fig.20), Moreover, we also observed that differently to circ-31, sometimes circ-16 joins SGs where only TIAR is present, suggesting that in this case the presence of FUS is not required for circ-16 SGs recruitment. However, also for circ-16, the topology of the interaction between

TIAR and circ-16 spots is predominantly in proximity (graph in Fig.20).

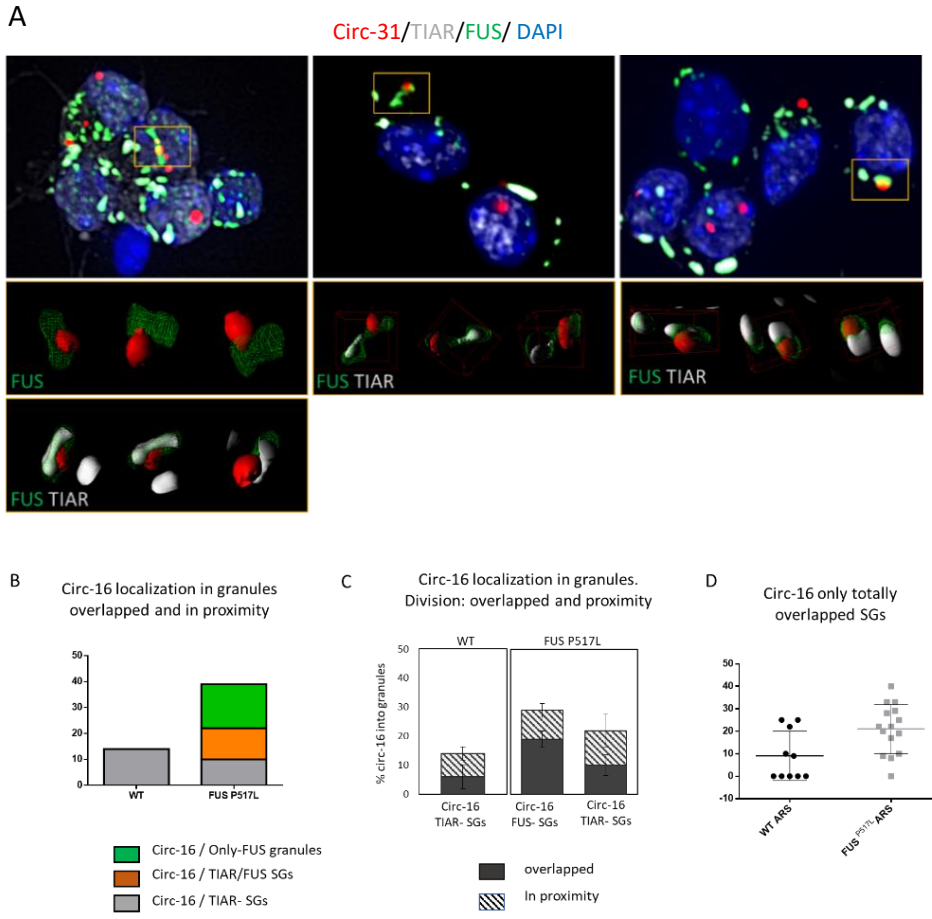

Figure20: A) Circ-16 staining in FUS P517L ARS cells, where the circRNA goes into SGs but with a different trend from circ-31. B) Counts of circ-16 in SGs, in proximity and overlapping spots together show 40% of circ-16 in SGs; C) Division among totally overlapped spots and spots in proximity, separately with FUS and TIAR, shows that a big part of the spots counted are in proximity (mean plus standard error are shown). D) ComDet and manual counts of only overlapped spots show no significant difference among WT and FUS P517L cells (scatter plot of percentages obtained by different images analysed; mean and standard deviation are shown).

To summarise:

1) in WT cells the presence of circ-31 into SGs is lower compared with FUS P517L cells upon the same stress conditions;
2) in FUS mutated cells circ-31 frequently localizes into SGs and FUS aggregates upon stress condition, and the topology of the granule suggests that circ-31 is mainly connected to FUS.
3) Circ-16 also localizes in SGs, preferentially staying in proximity and not totally overlapping, and sometimes also colocalizing with TIAR.

Overall, the results presented in this thesis strongly suggest a physical connection between circ-31 and the mutant isoform of FUS under oxidative stress.

3.4 Delving into the function of circRNAs: work in progress

For the functional study we focused on circ-31 and we exploited different approaches. In general, the study of circRNA function is challenging, mainly because the full sequence of the circular molecule is also present in the linear isoform, and only the backsplicing region can be used to discriminate between the two. With this in mind, several approaches have been employed to study the function of circ-31: 1) the Knock Down of circ-31 was obtained using siRNAs that specifically target the back-splicing junction; 2) the Knockout of circ-31 is achieved by the deletion of one of the two introns mediating circularization using the CRIPSR/Cas9 technology; 3) RNA pull down using antisense biotinylated oligonucleotides coupled with MASS-spectrometry and RNA-seq analyses in order to identify protein and RNA interactors respectively.

3.4.1 Knock down and Knock out

In order to knock down circRNAs we designed probes against the backsplicing junction that can specifically target the circular and not the linear isoform. We transfected MNs-d1 (1 day after dissociation at EBs d6) and we collected the cells for RNA extraction 48 hours later. The expression of both circular and linear isoforms upon circ-31 KD was measured using quantitative real time PCR (Fig.23). Total RNA from these experiments (n=3) was subjected to 3'UTRs RNA-Seq in order to determine if circ-31 down regulation might cause alterations in gene expression. Analysis of RNA-Seq data revealed that only few genes resulted to be altered in circ-31 KD condition (Fig.22). However, by performing Gene Ontology (GO) enrichment analysis using the "Gorilla" online tool we found genes belonging to the following functional categories: startle response, maintenance of protein localization and neuromuscular processes.

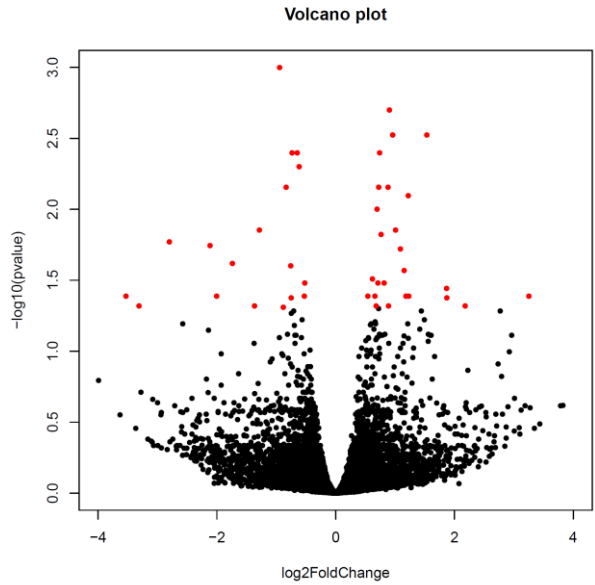

Description	P-value	FDR q-value	Enrichment (N, B, n, b)
startle response	5.93E-5	8.31E-1	38.46 (11768,17,54,3)
maintenance of protein location in cell	1.93E-4	1.00E+00	13.84 (11768,63,54,4)
sequestering of actin monomers	2.05E-4	9.56E-1	87.17 (11768,5,54,2)
maintenance of location in cell	3.78E-4	1.00E+00	11.62 (11768,75,54,4)
maintenance of protein location	7.24E-4	1.00E+00	9.79 (11768,89,54,4)
neuromuscular process	8.21E-4	1.00E+00	9.48 (11768,92,54,4)

Figure 22: volcano plot showing a trend of differentially expressed genes. In red: significantly altered RNAs. Few candidates have interesting fold changes.
Table 2: GO performed with the Gorilla online tool on RNAs differentially expressed upon circ-31 siRNA.

So far, we are currently working to validate these results and have noticed that the alteration of the targets has a strong variability among the different replicates where, unfortunately, we have a different effect of the siRNA also on the linear counterpart. Therefore, we are planning to perform siRNA against the linear isoform in order to determine what the targets affected by circ-31 and not by the

downregulation of the linear transcripts (Fig.23a) are. Moreover, it must be taken into consideration that due to the poor survival of sorted MNs after transfection, the siRNA transfections were performed using a mixed population of neuronal cells where the MN abundance is not greater than 25-30%. Therefore, the variability observed between replicates might be ascribed to the variation in the composition of the mixed population (interneurons, astrocytes and glial cells).

To overcome this problem, we set up a strategy to generate circ-31 KO mESCs in order to analyse the effect of a circRNA KO directly on sorted MNs. The approach consists in using the CRISPR/Cas9 technology to cut off one of the two flanking introns that are involved in circularization of the molecule. We decided to cut off the first intron since the deletion of the other one would have altered other linear isoforms with different termination codons. The strategy was to clone different sgRNAs in a plasmid also containing the coding sequence of the Cas9 endonuclease in order to obtain the co-expression of Cas9 and sgRNAs. We designed 4 sgRNAs targeting exon 1 (3') and exon 2 (5') and several sgRNAs targeting the intron, since it is 28 kb long and only two sgRNAs were not enough to efficiently remove the portion of DNA. Then, we used a dsDNA donor, thus a plasmid with two long homology arms, 800 nt each in length with a selection cassette between them (such as resistance to Puromycin and Blasticidin antibiotics) which is also flanked by inverted repeat sequences (IR), subsequently recognisable by a transposase enzyme (Fig23b). With this approach, we could select the cells where intron deletion and homologous recombination had occurred. Subsequently, the cassette can be removed by taking advantage of the transposase that recognizes the IRs. These two steps are needed to restore the exact sequence of exon1 and exon2. The necessity to use a DNA donor is related to the maintenance of the linear isoform. The cut generated within the genome can also be repaired by non-homologous end joining (NHEJ), which can introduce or remove nucleotides, altering the frame. Using the DNA donor with homology arms we can favour the homologous recombination rather than NHEJ. Clonal selection for mESCs resistant to Puromycin and/or Blasticidin is still ongoing. Regardless

the precautions taken, this type of genome editing could of course alter the expression of the linear counterpart, and in order to take this into account, the goal is to consider both KD and KO results when analysing alterations in gene expression.

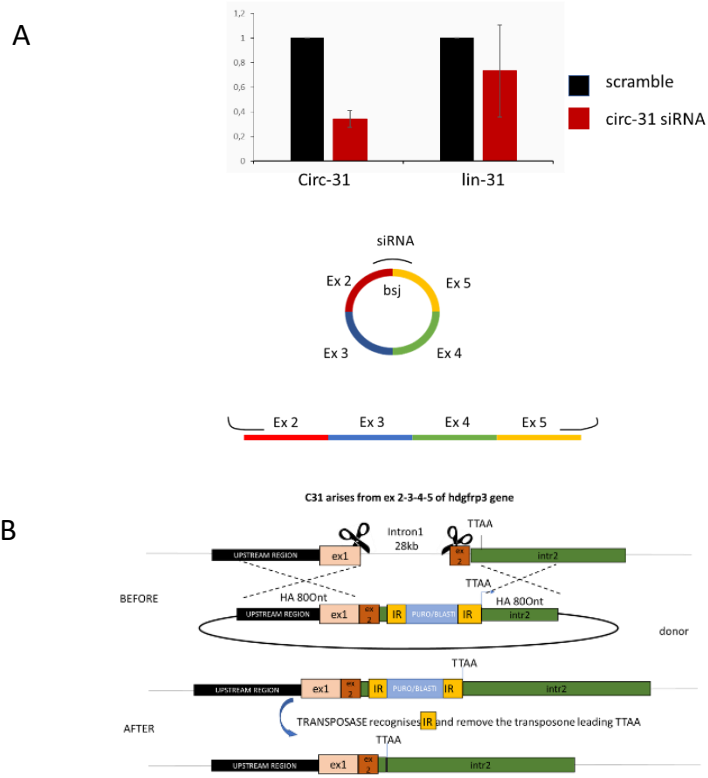

Figure 23: A) KD approach with the expression level of circ-31 and lin-31 upon circRNA KD. Lin-31 has a large standard deviation Bar due to differences arising among the biological replicates concerning linear-31 expression (N=4). B) KO approach comprising the use of Crispr/Cas9.

3.4.2 Finding interactors: circRNA Pulldown

The analysis of protein and RNA interactors is a good starting point in order to study the function of circRNAs. We performed two different types of circRNA pulldown to specifically identify protein or RNA interactors. To study circRNA-Protein interactions, we dissociated the EBs into single cells at the end of the MN differentiation (d6) and crosslinked them in suspension immediately after the dissociation, with UV (254 nm wavelength). We then prepared cellular extracts and performed the pulldown using 20 nt long biotinylated probes divided into two sets of four probes we called ODD and EVEN. We also used one type of probe only (1 probe circ) spanning the backsplicing junction (bsj). The ODD set had all the 4 probes in common with the linear isoform while the EVEN set had one of the probes on the bsj, thus specific for the circRNA. We also tested one probe only, specific for the linear isoform (1 probe lin) (Fig.24A). For the study of the RNA interactors we dissociated the EBs and plated them as a mixed population, performing an AMT-crosslinking step the following day. AMT (4'-aminomethyl-4,5',8-trimethylpsoralen) is a chemical compound which forms covalent bonds on amide base-pairing RNA molecules after UV-irradiation at 365 nm; the covalent crosslinking is revertible under UV-irradiation at 254 nm. Next, we performed the pulldown using the same set of probes as described above, except for 1 probe specific for the linear isoform. Figure 24 shows that when using ODD and EVEN sets, the linear isoform is also always pulled down along with the circular, since some probes are in common. For the 1 probe circ, even if the enrichment is not particularly high, we have a better enrichment for circ-31 compared to the linear RNA. We decided to include the MASS-spectrometry and RNA-sequencing analyses of this sample too since it could help us discriminate among proteins or RNAs that are specific for the circular molecule. Thus, we purified proteins at the end of the pull down with the UV-crosslinking and RNA from the pull down with psoralen-crosslinking.

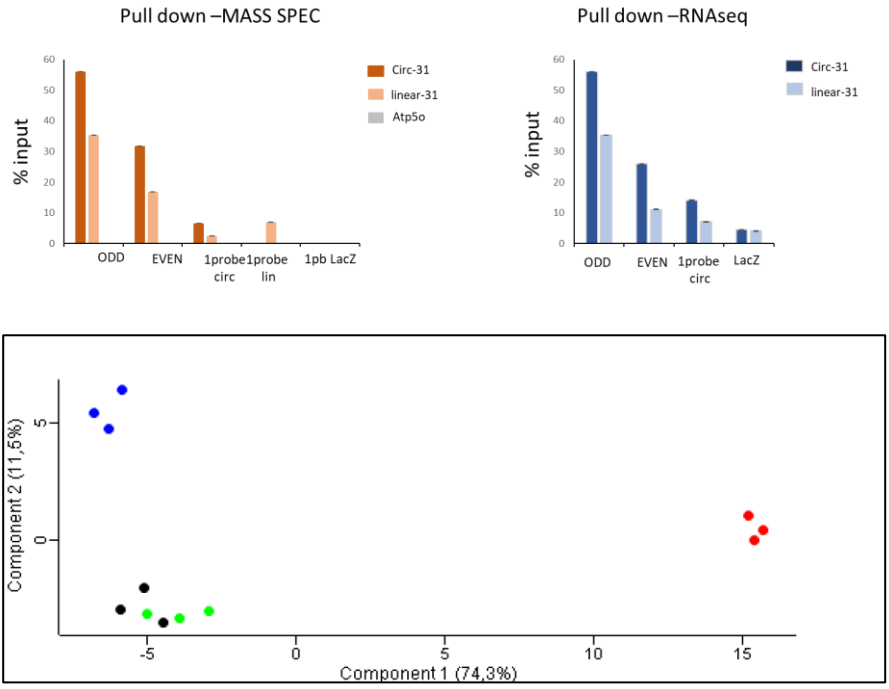

Figure24: A) circular and linear enrichment after the UV-crosslinked pulldown and AMT-crosslinking pulldown. B)PLA from MASS-spec shows EVEN (blue) and 1probe (green) have similar components, while ODD (red) is further away. The LacZ control is in black.

From the Mass-spectrometry results, we obtained a short list of proteins that could be good candidates. Interestingly, the EVEN set and ODD set are very different, while EVEN set has common features with the 1 probe set (Fig.24B). Validation of the interactors is still ongoing, however it is interesting to notice that among the putative interactors there is Annexin A2 that is involved in vesicular trafficking[154] suggesting that this protein might be responsible for circRNA transport.

With regards to the RNA interactors, the GO enrichment analysis shows that the recovered RNA belongs to the chromatin remodelling

and gene silencing categories (Fig.25). The interaction of circ-31 with RNAs involved in chromatin regulation and silencing lets us speculate about a possible role in the regulation of the translation of these mRNAs at the cytoplasmic level and in parallel the putative interaction with annexin A2 suggests an active or passive involvement in vesicle trafficking.

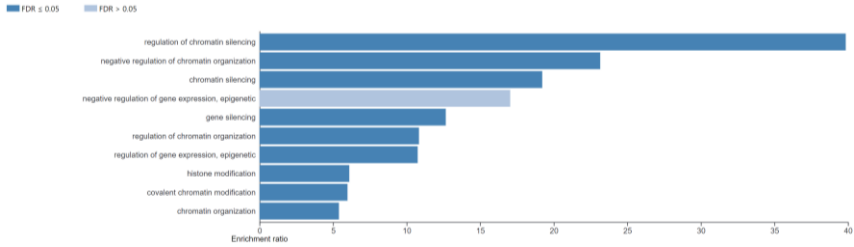

Figure 25: Gene ontology results with the webgestalt website.

4. DISCUSSION

In this thesis we analysed circ-31 and circ-16 subcellular localization through a new in situ hybridization (*ISH*) approach called Basescope™. The advantage of this approach is related to the possibility of targeting a small region and to amplify the signal. This is particularly convenient for the study of circRNAs, since they share all the sequences with the linear counterparts and the only region available in order to discriminate the two isoforms is the backsplicing junction (bsj). The protocol is based on the use of two Z-probes that we designed for the specific targeting of the 5' and 3' termini of the bsj. We optimised the protocol to be used on *in vitro*-derived MN cells, and we also succeeded in combining this *ISH* protocol with the immunofluorescence (IF) one. This allowed us to visualize circRNAs in cellular sub-compartments. We generated MNs from mESCs according to the Wichterle [151] protocol. In particular, we induced MN differentiation by activating the sonic hedgehog pathway and using retinoic acid. In six days, we obtained Embryoid Bodies that on the sixth day were disrupted in order to obtain single cells to plate. Cells derived by dissociated EBs are mixed neuronal cells (glia, interneurons, etc.) and around 20-30% of them are MNs[151 153 121].
In this mixed population, we carried out the Basescope™ assay combined with IF and we observed that while circ-16 was specifically present in ISLET-labelled MNs, in agreement with our previous results[56], circ-31 was also expressed in other neuronal cells. Moreover, we have noticed that circ-16 localises mainly in the soma and less frequently in the nucleus while circ-31 was also present in neurites. This is an interesting observation since the characteristic polarization of neuronal cells mirrors different functions for molecules localised in the soma with respect to those localised in neurites. Notably, we also showed that circ-31 localization in the neurites increases with MN maturation, suggesting a putative involvement in synapse formation/ regulation. Indeed, it was shown that mESC-differentiated MNs are able to establish synapses with muscular junctions in plates when cultured for at least 5-9 days with differentiated muscle cells, suggesting that MNs have to mature so as

to form active synapses[155]. The localization of circ-31 in different cellular contexts suggests the involvement of anterograde transport factors and also led speculations concerning a putative function that can be carried out in a synaptic context. Furthermore, we also decided to investigate the localization of circRNAs in other different cellular backgrounds. We employed mESCs carrying the FUS P517L mutation, corresponding to the human P525L FUS mutation. This latter resides on the NLS of FUS and affects its nuclear localization thus causing a massive increase of mutant FUS in the cytoplasm. Indeed, this mutation is linked to one of the most severe forms of familial ALS[118], that also presents FUS cytoplasmic inclusions. When mESCs carrying the FUS P517L mutation were differentiated into MNs, they did not show any differences in differentiation efficiency with respect to the WT condition[121]. Since circ-31 and circ-16 expression is affected in FUS KO MNs [56] we decided to verify whether in this condition, FUS mutations could alter circRNA localization, given that this protein is also involved in RNA export and transport. *ISH* on mutant cells did not show any alterations in the number of spots per cell or alterations in circRNA localization. Indeed, we observed circ-16 in the soma and nucleus and circ-31 in the soma and neurites with the same frequencies of WT cells. Thus, we decided to investigate whether oxidative stress conditions could affect circRNA localization. We focused our attention on circ-31 because of its fascinating localization in neurites under normal conditions. We have shown that oxidative stress, obtained by arsenite treatment; compromises circ-31 localization both in WT and mutant cells, induced a decrease of the molecule in the neurites and increases the retention in the perinuclear region. This result suggests that this retention could be due to an impairment of circRNA movement or due to an active retrograde transport upon stress. In order to answer this question, we decided to analyse the localization of the circRNA with respect to stress granules. These membrane-less organelles are ribonucleoparticles formed under different cellular stress conditions and represent a block of translation, required by the cell in order to contrast the stress[140] [156]. For the IF protocol we used anti-TIAR antibodies to mark SGs since TIAR is a master regulator of SG formation [131] and at the same time we also use anti-FUS antibodies

to stain FUS granules that frequently join SGs in FUS mutant cells [150] [127] [147] . In oxidative stress conditions we occasionally detected circ-31 close to SGs in WT cells, mainly in close proximity and rarely totally overlapping with TIAR. The presence of circ-31 close to SGs in WT cells is not as prominent as in FUS P517L cells, where almost 40% of circ-31 spots are detected in SGs. These findings suggest that the presence of circ-31 in SGs was somehow dependent on the presence of mutant FUS; this was also corroborated by the observation that circ-31 in mutant cells was likewise detected in FUS-granules where TIAR was not present. Interestingly, circ-16 showed a different behaviour since it was detected close to SGs also in the absence of cytoplasmic FUS; meaning that what was observed for circ-31 is not a general phenomenon. We also used different approaches, both computational and manual to determine the degree of proximity amongst circ-31 and SGs. Subsequently, we defined two main categories: spots in proximity and spots totally overlapped with SGs, and for each analysis TIAR and FUS were considered in an independent manner. We established that circ-31 is frequently overlapped with FUS and is preferentially in close proximity with TIAR in mutant cells. These results strengthen the hypothesis that FUS P517L has a role in the recruitment of circ-31 into SGs and FUS-only granules upon stress conditions. Moreover, it has been recently[157] shown that FUS mutations affecting FUS-RNA interactions are mainly arginine-affecting mutations (such as R216C, R244C, R514G, R521C, and R521G), while mutations in the NLS , such as FUS P525L/P517L, resemble FUS-WT in all aspects of RNA binding. This agrees with our observation, since circ-31 localization does not show any variation between FUS WT and FUS P517L conditions. However, under oxidative stress conditions, circ-31 is retained in the soma and we can hypothesize that in this condition the binding affinity of FUS changes, thus becoming sticky and able to trap circ-31. Another possibility is that this retention mechanism relies on an additional interactor that during stress is recruited in SGs in a FUS-dependent manner. This interactor could be a component of P-bodies as SGs and P-bodies dynamically interact fusing and splitting in a dynamic balance in different cellular conditions[128]. They also share proteins and mRNAs, among the latter mainly those that

are released from disassembled polysomes, sorted and remodelled at SGs and delivered to PBs for degradation. Mutant FUS tends to localize into SGs more than in PBs[115] but in 2014, Shelkovnikova and co-workers demonstrated that cytosolic FUS can aggregate with SGs through different steps: starting from RNA-dependent self-aggregation, passing through FUS-granule conditions (in cytosol without stress or very low levels) to FUS-aggregate conditions (upon stress). FUS aggregates co-localize with SG markers, although Shelkovnikova showed that FUS aggregates are inclusions that are different to SGs in origin, and can also localize with PB markers such as DCPB1[142]. Notably, our data shows that part of FUS granules do not colocalise with TIAR. In normal conditions, PBs are spread in different regions of the cell, including neurites, however in stress conditions they are closer to SGs, with a fraction of them being overlapped with SGs and part in close proximity[137 158 138]. This is similar to the spatial localization of our circRNAs. Thus, in this scenario a putative connection between circ-31 and PBs could explain the retention of circRNAs in the peri-nuclear region in WT cells treated with arsenite, since in this condition no localization of circ-31 with SGs has been detected. In mutant cells, the presence of FUS in the cytoplasm, already known to alter SG composition affects circ-31 localization, increasing the number of molecules joining SGs. Circ-31 in this condition might shuffle between PBs and SGs, and this could explain the different topological structures, proximity versus overlapping, where proximity spots could be in PBs. Therefore, our future perspective is to check by *ISH* and IF whether circ-31 is close to PB proteins. For circ-16, we can conclude that FUS is involved in this re-localization only in part, where we mainly see increases in circRNA proximity to both TIAR and FUS in mutant conditions.

We also wanted to investigate the function of circRNAs, despite it still being a challenging topic to address. The identification of circRNA interactors is a way to investigate circRNA function and many approaches have been developed so far: for instance, the circRNA pulldown coupled with mass spectrometry and RNA sequencing; crosslinking and immunoprecipitation (CLIP), RNP-immunoprecipitation (RIP) and so on[159]. Due to the presence of

circularising exons also in the linear transcripts, *in vitro* experiments can be carried out by incubating either circRNA or its linear counterpart with a putative protein interactor in order to establish whether the protein is a specific interactor of the circular molecule[72]. The treatment with RNAseR exonuclease of cell lysates, is an additional step that can be used to enrich the samples of circRNA specific interactors[68] by removing the linear RNAs. However, this treatment does not allow the identification of possible interactions between the linear and circular transcripts, since the possibility that circRNAs can bind linear RNAs cannot be excluded, probably by acting as scaffolds in order to mediate the interaction with proteins. It has been largely demonstrated that circRNAs can interact with small RNAs, such as miRNAs[160 77] and snRNAs[64] but there is no evidence of circRNAs interacting with long RNAs. Despite that, we decided to avoid the RNAseR treatment to carry out all the experiments presented in this thesis, in order to include any possible involvement of linear counterparts in circRNA function/interaction. Moreover, we should not underestimate the function of the circ-31 linear counterpart in neuronal cells. Hdgfrp3 is the only isoform of HDGFRP proteins that is specifically expressed in the neuronal system and it has been demonstrated to be required for neurite outgrowth, synaptic plasticity and is also secreted in cerebrospinal fluid (CSF)[161]. Indeed, HDGFRP3 is cytoplasmic and secreted at the early stages of hippocampal neuron development while in the adult brain it remains in the nucleus. Moreover, HDGFRP3 is also expressed and secreted in the spinal cord, where it exerts a relevant function for neuronal survival after nerve injury[162]. In addition, it has recently been found that HDGFRP's HATH domain, is also involved in DNA binding: it binds preferentially to H3K36me3/2 and it is involved in DNA repair[163]. The mechanism underlying the shuttling between nucleus and cytoplasm in different cell types is still unclear so far. One interesting scenario could be the involvement of circ-31 in the regulation of the HDGFRP3 mRNA, in its transport or translational regulation along neurites, since, as demonstrated in this thesis, circ-31 moves along neurites as well as HDGFRP3 mRNA (data not shown). In order to identify circ-31 interactors, we performed an RNA-pulldown and identified protein and RNA

molecules through mass spectrometry and RNA sequencing. Among protein interactors, we found annexin A2, a protein involved in cellular trafficking. Thus, one hypothesis could be the involvement of A2 in the circ/linear transport. In order to determine whether circ-31 and its corresponding mRNA interact with each other, an RNA *ISH* of both the molecules will be performed. In parallel we plan to check whether hdgfrp3 mRNA localization is affected in circ-31 Knock-down or Knock out conditions.
Interestingly, GO enrichment analysis of the transcripts identified in the RNA pulldown revealed that they belong to the chromatin silencing and histone modifications categories. Considering this result another scenario can be envisaged: circ-31 might be important for the post-transcriptional regulation of these genes or acting on the transport or on the stability.
In conclusion, we suggest a gain of function of cytoplasmic FUS P517L upon stress conditions, where the mutant protein induces a re-localization of circ-31. Considering that circ-31 might carry out a role at synaptic level or is involved in molecule trafficking by acting as cargo, its retention in pathological granules might represent another feature of ALS pathology related to FUS mutations.

5. MATERIALS AND METHODS

5.1 mESC differentiation into MNs

mESCs were cultured and differentiated into spinal motoneurons (MNs) as described in Wichterle's protocol of 2008[151]. mESCs were cultured with Embryomax MEM (Chemicon, cat. no. SLM-220-B), ES cell tested fetal bovine serum (FBS; HyClone, cat. no. SH30070.03), 100X Nucleosides (Chemicon, cat. no. ES-008-D), 100× non-essential amino acids (Chemicon, cat. no. TMS-001-C), 10 ng/ml of Leukaemia Inhibitor Factor (Chemicon, cat. no. ESG1107); FGFR inhibitor 1μM final concentration (Merk PD173074), GSK-3 inhibitor 0.1 μM final concentration (Merck 361559), plus 1% GlutaMAX, 1% 2-mercaptoethanol, 1% Pen/Strep. Generation of embryoid bodies (EBs) was obtained by culturing mESCs in ADNFK medium (1:1 Advanced DMEM/F12:Neurobasal medium, 10% Knock Out Serum Replacement (Gibco, 10828028), 1% GlutaMAX, 1% 2-mercaptoethanol, 1% Pen/Strep). On day 2, ADNFK medium was complemented with 2% B27 Supplement (Gibco, 17504-044), 1μM RA (Sigma Aldrich, R2625) and 0.5 μM SAG (Merck Millipore, 566660). EBs were expanded and then disrupted with Papain dissociation system (Worthington Biochemical Corporation) following the manufacturer's instructions. The mixed population of MNs was plated on Poly-L-ornithine (Sigma P3655) 1% and Laminin, 1% (Sigma L2020), eventually on glass slide for experimental analysis. Mixed populations were kept in culture with N2B27 with 1% N2 Supplement, 2% B27 Supplement medium, 1% Non-essential amino acids; neurotrophic factor BDNF (20 ng/ml final), GDNF(10ng/ml final), CNTF (10ng/ml final), 200 ng/ml L-ascorbic acid (Sigma-Aldrich) (TMS-001-C) (1% GlutaMAX, 1% 2-mercaptoethanol, 0.5% Pen/Strep).

5.2 Stress treatment and cell fixation

Cells were stressed with 0.5 mM Arsenite around 36 hours after being plated on PLO/Lam, for 45 minutes if used for experiments concerning the counting of circRNA in neurites, or for 1 hour if used for SGs localization analyses. Then, cells were fixed in 4% paraformaldehyde for 30 minutes at 4°C and washed twice with PBS. Subsequently we performed an alcoholic series: addition of ethanol at the following increasing concentrations: 50%-70%-100%, which was performed in an opposite, decreasing order prior to the start of the *ISH* experiments.

5.3 *ISH* and IF

For the *ISH*, we ordered two custom Z probes from Basescope™, by providing them with the region of the backsplicing junction (bsj) for circ-31 and circ-16.
For the linear RNA we used probes mapping on the canonical splice junction not included in the circRNAs, exon 5-6 of Hdgfrp3 mRNA for lin-31, and exon1 and exon2 for lin-16. BaseScope™.

Target	Catalogue number
mouse circ-31	cod. 703021
mouse lin-31	cod. 716031
mouse circ-16	cod. 708481
mouse lin-16	cod. 708491
negative control Dapb	cod. ef191515

Circ-31 bsj:
(ATTGATGAACTCCCAGAGGGTGCAGAAAGCCGGTGAAGG)
Circ-16 bsj:
(TCAGACTGCGCAAGAGAAAGTGGACAACATGGCAGATCAC)

For the *ISH* protocol we followed all the procedures described by the Basescope™ online protocol (https://acdbio.com/basescope). Briefly, this kit provides the two Z-like probes that must be incubated for 2h at 40°C. Subsequently, we performed 8 steps of different probe

incubation alternated by washes (wash buffer provided by Basescope™). At the end of all the incubation steps we used fast-red to detect the signal. Differently from the Basescope™ kit's canonical protocol we set up the protease III pre-treatment condition at a 1:15 dilution, for our cells. At the end of the *ISH* protocol, we performed the immunofluorescence steps. We then performed a blocking step in PBS with 2% BSA, and subsequently performed primary antibody incubation overnight at 4°C and 45 minutes of secondary antibody incubation. DAPI (Sigma-Aldrich) was used to label nuclei.

Primary antibodies	**Concentration**
Mouse Anti-FUS/TLS SC 47711 (mouse monoclonal) recognizes C-terminus	1/200
Mouse Anti-FUS Ab84078 (Rabbit polyclonal) recognizes region within the amino acids 1-50	1/200
Mouse Anti-TIAR S BD 610352 (mouse)	1/200
Mouse Anti-ISLET 1/2 394D5 (mouse)	1/50
Mouse βTUJI (anti-Tuj1) (Sigma T2200) (Rabbit)	1/200
Secondary antibodies	**Concentration**
Goat anti-Mouse IgG (H+L) Highly Cross-Adsorbed Secondary Antibody, Alexa Fluor 488 Thermof FISHer Catalog #: A-11029	1/200
Donkey anti-Rabbit highly cross-adsorbed alexa fluor 647 thermof FISHer cod. A32795	1/100
Goat anti-Rabbit IgG (H+L) Cross-Adsorbed Secondary Antibody, Alexa Fluor 488 Thermof FISHer cod. A-11008	1/200

Table 3: list of antibodies used

Confocal images were acquired using an inverted Olympus iX73 microscope equipped with an X-light Nipkow spinning-disk head (Crest Optics) and Lumencor Spectra X LED illumination. Images were collected using a CoolSNAP MYO CCD camera (Photometrics)

and MetaMorph software (Molecular Devices) with a 60X oil objective. For RNA *ISH* and IF the Z-stack confocal microscopy images were taken automatically (0.2-µm path) and merged with maximum intensity projections to obtain 2D images, or processed for image analysis. In this latter case a Laplacian-of-Gaussian filter was applied to a 3D volume after image acquisition to enhance the spot signal over the background [164]. The intensity threshold was manually adjusted using the ImageJ software. Signal from cells hybridized with negative control probes was considered as background. The co-planarity and the co-localization of the RNA spots and TIAR or FUS protein were established by recording the main gray scale value (expressed as arbitrary units, slice or µm) along Z-planes using ImageJ (Plot *Z*-axis profile) (Fig.20b). The percentage of circ-31 spots localizing with FUS and/or TIAR were firstly obtained with the ComDet plugin for finding and analysing colocalization of bright intensity spots (cells, particles, dots, etc). The plugin works with z-stacks and detection can be performed in a specific region or in the whole image, provided that for an image containing two-colour channels is supplied for colocalization. We set the particle intensity threshold to 50 SD and an approximate particle size to 7.00 pixels for both channels to permit aggregate recognition. We corrected the ComDet count by manual screening, analysing single focal planes. Spots showing spatial proximity or totally overlapping were determined by 3D Object count, where proximity distance was 0.66 µm and overlapping < 0.66 µm. Moreover, Pearson's correlation coefficient was obtained by using the Jacob plugin and it was <0.2 for "in- proximity" spots and > 0.2 for "overlapping" spots.[165] The Jacob threshold to binarize the images and needed to calculate Pearson's coefficient was set for each single image to remove the background signal and maintain only the granule/circRNA signal. 3D rendering was performed with the 3DViewer plugin. We firstly set scale (for 60X magnification=13,333 pixel/µm) and then we set pixel width and height to 0.075 µm, and voxel depth to 0.20 µm. Eventually we processed SGs and circRNA spots with the Gaussian Bluer 3D processing tool, in order to make object surfaces more homogeneous, and subsequently displayed image with a surface view.

Statistical analyses on counts were obtained through non-parametric tests using GraphPad prism. In the graph, we showed results for one representative experiment where N= percentage obtained in each image acquired. Number of spots was shown below each experiment.

5.4 siRNA design and transfection

We designed siRNA against circ-31 using the Dharmacon online tool and we provided the backsplicing junction. We employed ON-TARGETplus siRNA against circ-31 and against a scrambled RNA (ON-TARGETplus Non-targeting Pool # D-001810-10-20).
Circ-31 siRNA:
Sense:5'CGGUGAAGGGAUUGAUGAAUU3'
Antisense: 5' UUCAUCAAUCCCUUCACCGUU 3'
Motoneurons (MNs) where transfected one day after dissociation. We used 5µl of RNAiMAX Transfection Reagent, 300 µl of Opti-MEM™ (both Sigma/Aldrich), and 50 µM of siRNA, incubating them together for 20 minutes. Subsequently, we added the mix on plated MNs, with 1.7 mL of MN medium (N2B27), in a final volume of 2 mL in p35 mm plates containing 1 million MNs. We changed the medium one day later (overnight transfection) and we finally collected the cells and extracted RNA after 48 hrs from the transfection.

5.5 RNA extraction, quantification and reverse transcription

Cells were washed with PBS without Ca^{2+} and Mg^{2+} and detached by using Qiazol reagent (Qiagen), a mono-phasic solution of phenol and guanidine isothiocyanate. RNA extraction was then performed with the Qiagen RNeasy Mini Kit according to the manufacturer's indications and subsequently, RNA concentration was measured with NanoDrop 1000 Spectrophotometer. For testing siRNA efficiency, we performed reverse transcription using the PrimeScript™ RT Reagent Kit (Takara) according to the manufacturer's protocol, in a final reaction volume of 10 µL.

5.6 siRNA sequencing and Gene Ontology

RNA sequencing for circ-31 siRNA experiments was performed in Ngs core of Tigem in Naples through Quantseq 3' DGE sequencing that employs a QuantSeq Library kit for 3' UTR RNA library preparation and Illumina sequencing. Bioinformatic analyses were done by the Bioinformatic facility of Tigem by employing the edgeR R-Biocondictor package. Selected RNA candidates have an FDR < 0.05-0.1. Gene ontology was performed by using the Gorilla online tool.

5.7 CRISPR/ cas9 cloning and transfection

We employed the PX333 plasmid containing Cas9[166] and we cloned sgRNA guides in order to perform double strand breaks on Hdgfrp3 genes. sgRNA used where designed and cloned following Zhang's protocol [167]. sgRNA map at exon1-intron1 splice junction and intron1-exon2 splice junction of the Hdgfrp3 gene.

sgRNA used:
c31-sgRNA-1E-FWD CACCGCCCGCCCGGGTGAGTACGG
c31-sgRNA-1E-REV AAACCCGTACTCACCCGGGCGGGC

c31-sgRNA-2E-FWD CACCgAATAATTGATGAACTCCCAG
c31-sgRNA-2E-REV AAACCTGGGAGTTCATCAATTATTc

c31-sgRNA-1G-FWD CACCgCTACCCGCACTGGCCCGCCC
c31-sgRNA-1G-REV AAACGGGCGGGCCAGTGCGGGTAGc

c31-sgRNA-2G-FWD CACCTTTGTTAACTTACGTTTCAT
c31-sgRNA-2G-FWD AAACATGAAACGTAAGTTAACAAA

We also employed three sgRNA transcribed *in vitro* (according to the manufacturer, Guide-it™ sgRNA *In Vitro* Transcription and Screening Systems) targeting internal regions of intron1, respectively at 1,2- 10-20 kb from the exon1-intron1 junction:
Intr1-1,2 FWD TGTGAGCATCCACTTCTGTGTTTG

Intr1-1,2	REV	TGGCGAGGATGTGGAGAAAGA
Intr1-10	Fwd	TAACCTTCCCCATCAATCAAAAC
Intr1-10	REV	TGGAGTCCCTTCTTCTTTGTTGA
Intr1-20	FWD	ACCCTGTCTCAAAATACGAAACACT
Intr1-20	REV	TTGTCAGCTTCATAGATGCTTGGAC

The dsDNA donor, employed to allow the homologous recombination with the purpose of maintaining the frame after the Cas9 DNA double strand break, was cloned inserting homologous arms (HA, 800nt each one) flanking inverted repeat sequences (recognised by the transposase) containing a cassette composed by the CMV promoter (from-pcDNA3.1) upstream of Puromycin or Blasticidine resistance genes. Inverted repeat sequences were amplified from the ePB-puro-TT plasmid[168] [103]. The cassette was inserted in a specific region of exon2 (component of Has) presenting a TTAA site. This sequence will be recognised by a transposase that will remove the cassette without leaving a scar in the genome (scheme of the strategy in Fig 23.b)[169]. This allows the clonal selection of resistant clones (for puromycin and blasticidine) and the ssubsequent removal of the cassette allows the recovery of the correct reading frame without altering the basal expression of the linear isoform. Cloning was performed employing the In-fusion® kit, according to the manufacturer's protocol. Cloning with this approach requires the addition of a 15nt-long tail to the oligonucleotides, in order to create a homology region between the insert and plasmid, allowing recombination to take place inside bacterial cells (E.Coli STBL3®).

Main oligonucleotides used for cloning:

homology arm amplification in 3 PCR steps	
1- 5'upstream-exon1	
Tail*/F1	CGGTATCGATAAGCT-GGGCAGTCAGAAAGGGGGT
REV1	GCGACCGCAAACACGATCTTA
2-exon 1-exon 2	
F2 E1/E2	GATCGTGTTTGCGGTCGCTGCCCGAGGAGGAATTCGG

R2 E1/E2	CGGGCTGCAGGAATT-AGGGTACTTGTTTGCTGGAGGC
3- E2-intr2	
F1 E2/intr2	GCAAACAAGTACCCT-ATCTTCTTTTTTGGTACCCATGAAAC
R2 intr2/tail*	CGGGCTGCAGGAATT -ACGTGTGTACTACTGTGAAAGAAGGA
open HA to insert Puromycin or Blasticidin between IR sequences	
openHR-REV GCTATTTTGTTAACTTACGTTTCATG)	
openHR-FWD ATTTTTCAATAGCTCTAATTTGACTAC	

**tail is referred to the 15nt added to oligonucleotides in order to permit the homologous recombination between insert and plasmid.*

For mESC transfection we incubated 5 µL of Lipofectamine 2000, 1 mL of Opti-MEM, 1 µg of Donor plasmid, 1 µg in total for all the sgRNAs-cloned into the plasmids) and 50 nM of each sgRNA (in-vitro transcribed) for 30 min. Then we performed inverse the transfection with 250,000 mES cells and incubated them for 1h at 37°C before plating them.
Clonal selection of mESCs resistant for Puromycin and Blasticidine is still ongoing.

5.8 Pulldown

For the circ-31 pulldown we used 3' biotinylated probes (Sigma), hereby listed:

ODD	TACTTGTTTGCTGGAGGCTT
ODD	CCGTTTGTTTGACTTTCCAA
ODD	TGCTTGCATCTGCAGTATTT
ODD	GTCTTTATCATCTTCGTCTC
EVEN	GAGTTCATCAATCCCTTCAC
EVEN	ACTTGTCTTTGTATTCCTTA
EVEN	TCTGTTGCTGAATTGTCTGG

EVEN/ 1probe circ	AGGGATTGATGAACTCCCAG

5.8.1 UV-crosslink protocol

EBs were dissociated and maintained in suspension with 4 mL of Glucose-PBS buffer (4% glucose; 2,5% Horse serum, 2% B27) and then crosslinked with UV 4000 x 100 μJ/cm^2 energy (254 nm wavelength). We crosslinked around 300 x 10^7 cells. We extracted proteins using Lysis Buffer (Hepes 10mM; KCl 20 mM; $MgCl_2$ 1.5 mM; DTT 1mM; EDTA 0.5 mM, glycerol 20%, NP40 1%, Protease and RNase Inhibitor) and incubated on ice for 15 minutes. The cytoplasmic extract was recovered by centrifugation at 2000 rpm, 10 minutes, 4°C, and protein concentration was determined with the Bradford reagent assay. We performed the pulldown using 1.5 mg of proteins for each set of probes. Extract precleaning was performed with 50 μL of Streptavidin MagneSphere Paramagnetic Particles (Promega) equilibrated in Hybridization Buffer (Tris-HCl pH 7.5 100 mM; NaCl 500 mM; SDS 0.2% NP-40; 0,1%; EDTA 10 mM; DTT 1 mM; Protease and RNase Inhibitor) for 30 minutes in rotation at room temperature (R.T). Subsequently, 50 pmoles of a mix of four different biotinylated probes was added to each reaction (for the 1 probe we used 50 pmoles of the same bsj probe) and incubated for 2 hours in rotation at R.T to permit hybridization with the target. After the incubation, 100 μL of the magnetic beads were added in each sample and incubated for 30 minutes on the wheel at R.T, in order to pull down biotinylated probes/Target, and then we washed 5 times in 500 μL of Hybridization Buffer. The samples were divided into two aliquots, for RNA and protein analysis. The RNA fraction was resuspended in ProteinaseK Buffer (Tris-HCl pH 7 10 mM, NaCl 100 mM, EDTA 1 mM, SDS 0.5%) and heated for 2' at 95°C in order to remove the magnetic beads. Then 1 mg/mL of Proteinase K was added, and all the mix incubated at 52-55 °C to reverse the crosslinking, and finally we recovered the RNA by adding 5 volumes of QIAZOL. The protein part was collected to perform MASS-

spectrometry accordingly with RAP/MASS-SPEC protocol from Guttman[170]. Therefore, we resuspended the beads in Benzonase buffer (TrisHCl pH 8 20 mM, N-lauroylsarcosine 1M, 2 mM $MgCl_2$, DTT 0.5 mM) and then added 80 U of Benzonase and incubated for 2 hrs at 37°C with intermittent mixing (30 seconds) at 1100 rpm using a thermomixer. We removed the magnetic beads and finally performed TCA protein precipitation (10% final of TCA) overnight at 4°C and the day after, the samples were centrifuged at 16000 g for 30 minutes at 4°C. Precipitation was performed with cold Acetone followed by the last centrifuge of 15 minutes at 16000 g.
RNA was used to check input percentage of enrichment of circRNA and linear counterpart, and the extraction and reverse transcription were performed as previously described.
Proteins were used for MASS-spectrometry, which was performed in *Plateforme de Protéomique IGBMC (Strasbourg, France)*. There, the samples were prepared by liquid digestion (LysC/Trypsin) and mass spectrometry was performed using the Orbitrap ELITE instrument and C18 5O cm column with analyse method of TOP20CID, 2h run in triplicate. The Software *Identification Proteome Discoverer 2.2* was used for the analysis of results and for protein identification and *Perseus 1.6.6.0* for statistics.

5.8.2 AMT-crosslinking pulldown

EBs were dissociated and 40 million cells were plated on two PLO/LAM-coated p10 dishes. One day later, MN medium was replaced with cold PBS with 200 ug/mL of AMT (80 uL of 2.5 mg/mL stock solution) and crosslinked at 365 nm for 10 minutes. Then, cells were lysed in 1 volume of Guanidinium Hydrochloride 6M and the lysate was subdivided in aliquots by adding 20 mg/mL solution of RNase inhibitor, proteinase K (Ambion) and 20% sodium dodecyl sulfate (SDS) and then samples were incubated at 65°C for one hour at 400 rpm. Then, we added TRIZOL to each aliquot and performed RNA extraction as previously described and stored it at -20 °C. The day after we preheated the aliquots with 2x Binding Buffer (TRIS-HCl (pH 7.5) 10 mM, NaCl 500 mM, EDTA 1 mM, SDS 0.05 %) at 65°C and subsequently incubated the 40µg of RNA

with each specific set of probes (the same described previously). RNA was heated at 95°C for 3 minutes, then moved on ice and then we added the probes (50 pmoles). Samples were heated at 65°C for 5 min and we added 500 uL of preheated (2x) Binding Buffer and incubated for 4h on the wheel. Overnight, we incubated the samples with magnetic beads and the day after we performed washes on beads and a second Qiazol RNA extraction, concluding with reverse psoralen crosslinking using UV 254 nm for 10 minutes.
The Ovation RNA v2 followed by Ovation Ultralow v2 kit was used to prepare cDNA libraries for Pull-down RNA-Seq experiments. The sequencing reactions, performed on an Illumina NovaSeq6000 Sequencing system at the Institute of Applied Genomics (IGA; Udine, Italy), produced an average of 43.3 million 150 nucleotide long paired-end reads per sample. Reads were pre-processed using Trimmomatic software[171], which removed adapter sequences and poor quality bases. Alignment to the mouse GRCm38 genome and transcriptome was performed using STAR aligner[172]. The alignment file was further preprocessed by filtering out reads mapping to rRNAs and tRNAs, removing PCR duplicates using Picard MarkDuplicates (available at http://broadinstitute.github.io/picard) and discarding the multi-mapped reads using bam tools[173]. The Piranha tool was used to call peaks for circRNA Pull-down and LacZ Pull-down reads, using Input reads as a covariate. BEDtools[174] intersect tool was used to annotate circRNA Pull-down peaks based on their overlap with Ensembl 90 exons and to filter out transcripts hosting LacZ peaks. Common targets were further removed.

5.9 RealTime PCR and primers

Realtime PCR was performed to control pulldown target enrichment. We employed LifeTech Power-UP SYBERgreen and the 7500Fast instrument.

Linear-31	FWD GCGAGCAGGAGAACGACCG	REV TACTTGTTTGCTGGAGGCTTCA
Atp5o	FWD CAACCGCCCTGTACTCTGCT	REV GGATTCAGAACAGCCAGAGACAC
Circ-31	FWD AGACGCTGGCAATGACACGA	REV TACTTGTTTGCTGGAGGCTTCA
Linear-16	FWD CGTGACCTCAGCCAGCAATG	REV ATATGACACTCAAAGGGATGGAAGT
Circ-16	FWD CGTGACCTCAGCCAGCAATG	REV ATATGACACTCAAAGGGATGGAAGT

GLOSSARY

- **3D LoG filter (Laplacian of Gaussian):** is an available plugin able to apply a LoG filter to a 2D image or to 3D volume in order to enhance spots, like spherical particles, reducing noisy background. The module is easily tuned selecting the standard deviations in X, Y and Z directions, since the parameters σx, σy and σz define the size of the LoG filter.
- **3D Object count:** Is an ImageJ plugin that gives us the smaller distance between two spots, (the two mass centres), working on Z-stack, considering the distance also on the Z axis.
- **Backsplicing junction:** is the splicing junction arising from head-to-tail "backsplicing" of a down- stream 3′ splice site to a more upstream 5′ splice site.
- **"In Proximity" spots:** in our analysis, spots with a minimum distance of 0.66 μm and a Pearson's coefficient < 0.2 are considered in proximity.
- **ComDet**: is a plugin for finding and/or analysing colocalization of bright intensity spots (cells, particles, dots, etc) in images with a heterogeneous background. Plugin works with z-projection and detection can be performed in some specific regions or within the whole image, provided that for colocalization, an image containing two-color channels is supplied.
- **CRISPR/Cas9:** Is a genome editing approach based on the use of the Cas9 bacterial endonuclease, engineered to perform editing of any species' genome. The Cas9 can bind a specific sequence of a sgRNA. The remaining part of the sgRNA is designed to be able to recognise a region in the genome (pairing region is 20 nt). Thus, sgRNA bound to Cas9 brings the enzyme on a specific target region[175 176].
- **JACoP (Just Another Co-localization Plugin)**: is a toolbox for subcellular colocalization analyses under ImageJ. General overlay methods generate visual estimates of colocalization events in two-dimensional images. JACoP proposes to

compare the global statistic approaches that rely on intensity-correlation coefficient-based (ICCB) analysis and provides the possibility to process image stacks for an automated colocalization analysis in three-dimensions. We used JaCoP to generate Pearson's coefficient.

- **mESC WT and FUS P517L**: mouse embryonic stem cells were kindly provided by Neil A. Schneider and FUS mutated cells were taken from Knock in mice.
- **Neurites**: category that includes axons and dendrites.
- **P-Bodies**: processing bodies mainly composed of translationally repressed mRNAs and proteins related to mRNA decay, suggesting roles in post-transcriptional regulation.
- **Pearson's correlation coefficient**: index of co-occurrence of two signals based on pixel overlapping. We used it to characterize the degree of overlap between FUS- TIAR and circRNAs. The coefficient ranges from 1 to -1, where 1 stands for complete positive correlation, -1 for negative correlation and 0 for no correlation.
- **RNA pulldown:** molecular technique in which a specific RNA is pulled down, enriched from an input of extract, by using biotinylated probes.
- **RNA silencing (siRNA):** technical approach of molecular biology that employs anti-sense RNA to target an endogenous RNA, forming a dsRNA that is recognised by the cells which activate the RISC complex in order to induce RNA degradation. In our experiment, it is used to perform the Knock down of the molecule.
- **RNA-Seq: (**RNA sequencing) a technique used to identify and quantify RNA molecules altered in siRNA of circRNA and to identify RNA interactors after pulldown with psoralen (AMT) crosslinking. It is performed by using next-generation sequencing.
- **Soma:** cell body of the neurons excluding neurites.
- **Spinal Motoneurons (MN):** are neuronal cells that serve to innervate muscles. MNs and muscle fibres form

neuromuscular Junctions and the complexity of MN terminations with muscle fibres are called motor units. MNs release neurotransmitters, one of the most important being Acetylcholine (Ach), that is bound by the Ach-Receptor on muscle membrane.

- **Stress Granules (SG):** cytoplasmic aggregates of stalled translational preinitiation complexes that accumulate during stress. Their assembly requires eIF2alpha phosphorylation.
- **Synapses:** Cellular structures that connect neuronal cells and other neuronal cells or muscle cells. They serve to transmit impulses that can be chemical or electrical, based on the type of neurotransmitter. Normally, the presynaptic region is the region of the cells that transmits the signal and the post-synaptic region is the cell that receives the signal.
- **Synaptosomes:** subcellular fraction prepared from brain tissue containing large fractions of resealed postsynaptic entities fused to presynaptic portions of the synapse.
- **Totally Overlapped/Overlapped spot**: distance <0.66 µm and with a Pearson's coefficient >0.2.
- **Z-projection:** allows us to visualize Z-stack series (where stack is the image obtained for one single focal plane) as 2D images. Maximum intensity projection creates an output image each of whose pixels contains the maximum value over all images in the stack at the pixel location.

BIBLIOGRAPHY

1. Gros F, Hiatt H, Gilbert W, Kurland CG, Risebrough RW, Watson JD. Unstable ribonucleic acid revealed by pulse labelling of Escherichia coli. *Nature*. 1961;190(4776):581-585. doi:10.1038/190581a0
2. Jacob F, Monod J. Genetic regulatory mechanisms in the synthesis of proteins. *J Mol Biol*. 1961;3(3):318-356. doi:10.1016/S0022-2836(61)80072-7
3. Kruger K, Grabowski PJ, Zaug AJ, Sands J, Gottschling DE, Cech TR. Self-splicing RNA: Autoexcision and autocyclization of the ribosomal RNA intervening sequence of tetrahymena. *Cell*. 1982;31(1):147-157. doi:10.1016/0092-8674(82)90414-7
4. Lee RC, Feinbaum RL, Ambros V. The C. elegans heterochronic gene lin-4 encodes small RNAs with antisense complementarity to lin-14. *Cell*. 1993;75(5):843-854. doi:10.1016/0092-8674(93)90529-Y
5. Fire A, Xu S, Montgomery MK, Kostas SA, Driver SE, Mello CC. Potent and specific genetic interference by double-stranded RNA in caenorhabditis elegans. *Nature*. 1998;391(6669):806-811. doi:10.1038/35888
6. Wilusz JE, Sunwoo H, Spector DL. Long noncoding RNAs: Functional surprises from the RNA world. *Genes Dev*. 2009;23(13):1494-1504. doi:10.1101/gad.1800909
7. Ulitsky I, Bartel DP. XLincRNAs: Genomics, evolution, and mechanisms. *Cell*. 2013;154(1):26. doi:10.1016/j.cell.2013.06.020
8. Rinn J, Guttman M. RNA and dynamic nuclear organization. *Science (80-).* 2014;345(6202):1240-1241. doi:10.1126/science.1252966
9. Dunham I, Kundaje A, Aldred SF, et al. An integrated encyclopedia of DNA elements in the human genome. *Nature*. 2012;489(7414):57-74. doi:10.1038/nature11247
10. Palazzo AF, Lee ES. Non-coding RNA : what is functional and what is junk ? 2015;6(January):1-11. doi:10.3389/fgene.2015.00002

11. Yashiro R, Murota Y, Nishida KM, Negishi L, Siomi H, Correspondence MCS. Piwi Nuclear Localization and Its Regulatory Mechanism in Drosophila Ovarian Somatic Cells. *Cell Rep*. 2018;23:3647-3657. doi:10.1016/j.celrep.2018.05.051
12. Matera AG, Terns RM, Terns MP. Non-coding RNAs: Lessons from the small nuclear and small nucleolar RNAs. *Nat Rev Mol Cell Biol*. 2007;8(3):209-220. doi:10.1038/nrm2124
13. Rinn JL, Chang HY. Genome Regulation by Long Noncoding RNAs. doi:10.1146/annurev-biochem-051410-092902
14. Struhl K. Transcriptional noise and the fidelity of initiation by RNA polymerase II. *Nat Struct Mol Biol*. 2007;14(2):103-105. doi:10.1038/nsmb0207-103
15. Penny GD, Kay GF, Sheardown SA, Rastan S, Brockdorff N. Requirement for Xist in X chromosome inactivation. *Nature*. 1996;379(6561):131-137. doi:10.1038/379131a0
16. Plath K, Talbot D, Hamer KM, et al. Developmentally regulated alterations in polycomb repressive complex 1 proteins on the inactive X chromosome. *J Cell Biol*. 2004;167(6):1025-1035. doi:10.1083/jcb.200409026
17. Clemson CM, Hutchinson JN, Sara SA, et al. An architectural role for a nuclear noncoding RNA: NEAT1 RNA is essential for the structure of paraspeckles. *Mol Cell*. 2009;33(6):717-726. doi:10.1016/j.molcel.2009.01.026
18. Bond CS, Fox AH. Paraspeckles: Nuclear bodies built on long noncoding RNA. *J Cell Biol*. 2009;186(5):637-644. doi:10.1083/jcb.200906113
19. Kretz M, Siprashvili Z, Chu C, et al. Control of somatic tissue differentiation by the long non-coding RNA TINCR. *Nature*. 2013;493(7431):231-235. doi:10.1038/nature11661
20. Faghihi MA, Modarresi F, Khalil AM, et al. Expression of a noncoding RNA is elevated in Alzheimer's disease and drives rapid feed-forward regulation of beta-secretase. *Nat Med*. 2008;14(7):723-730. doi:10.1038/nm1784
21. Kang M-J, Abdelmohsen K, Hutchison ER, et al. HuD regulates coding and noncoding RNA to induce APP→Aβ processing. *Cell Rep*. 2014;7(5):1401-1409.

doi:10.1016/j.celrep.2014.04.050
22. Gong C, Maquat LE. LncRNAs transactivate STAU1-mediated mRNA decay by duplexing with 39 UTRs via Alu eleme. *Nature*. 2011;470(7333):284-290. doi:10.1038/nature09701
23. Hutvagner G, Simard MJ. Argonaute proteins: key players in RNA silencing. *Nat Rev Mol Cell Biol*. 2008;9(1):22-32. doi:10.1038/nrm2321
24. Cesana M, Cacchiarelli D, Legnini I, et al. A long noncoding RNA controls muscle differentiation by functioning as a competing endogenous RNA. *Cell*. 2011;147(2):358-369. doi:10.1016/j.cell.2011.09.028
25. Hansen TB, Jensen TI, Clausen BH, et al. Natural RNA circles function as efficient microRNA sponges. *Nature*. 2013;495(7441):384-388. doi:10.1038/nature11993
26. Piwecka M, Glažar P, Hernandez-Miranda LR, et al. Loss of a mammalian circular RNA locus causes miRNA deregulation and affects brain function. *Science (80-)*. 2017;357(6357). doi:10.1126/science.aam8526
27. Sanger HL, Klotz G, Riesner D, Gross HJ, Kleinschmidt AK. Viroids are single stranded covalently closed circular RNA molecules existing as highly base paired rod like structures. *Proc Natl Acad Sci U S A*. 1976;73(11):3852-3856. doi:10.1073/pnas.73.11.3852
28. Kos A, Dijkema R, Arnberg AC, Van Der Meide PH, Schellekens H. The hepatitis delta (δ) virus possesses a circular RNA. *Nature*. 1986;323(6088):558-560. doi:10.1038/323558a0
29. Soma A, Onodera A, Sugahara J, et al. Permuted tRNA genes expressed via a circular RNA intermediate in Cyanidioschyzon merolae. *Science (80-)*. 2007;318(5849):450-453. doi:10.1126/science.1145718
30. Soma A. Circularly permuted tRNA genes: Their expression and implications for their physiological relevance and development. *Front Genet*. 2014;5(APR). doi:10.3389/fgene.2014.00063
31. Tang TH. RNomics in Archaea reveals a further link between

splicing of archaeal introns and rRNA processing. *Nucleic Acids Res*. 2002;30(4):921-930. doi:10.1093/nar/30.4.921

32. Danan M, Schwartz S, Edelheit S, Sorek R. Transcriptome-wide discovery of circular RNAs in Archaea. *Nucleic Acids Res*. 2012;40(7):3131-3142. doi:10.1093/nar/gkr1009
33. Grabowski et al. 1981 - Cerca con Google. https://www.google.com/search?q=Grabowski+et+al.+1981&rlz=1C1RNDG_enIT806IT806&oq=Grabowski+et+al.+1981&aqs=chrome..69i57.1268j0j4&sourceid=chrome&ie=UTF-8. Accessed October 28, 2019.
34. Nielsen H, Fiskaa T, Birgisdottir ÅB, Haugen P, Einvik C, Johansen S. The ability to form full-length intron RNA circles is a general property of nuclear group I introns. *RNA*. 2003;9(12):1464-1475. doi:10.1261/rna.5290903
35. Kjems J, Garrett RA. Novel splicing mechanism for the ribosomal RNA intron in the archaebacterium Desulfurococcus mobilis. *Cell*. 1988;54(5):693-703. doi:10.1016/s0092-8674(88)80014-x
36. Zhang Y, Zhang XO, Chen T, et al. Circular Intronic Long Noncoding RNAs. *Mol Cell*. 2013;51(6):792-806. doi:10.1016/j.molcel.2013.08.017
37. Nigro JM, Cho KR, Fearon ER, et al. Scrambled exons. *Cell*. 1991;64(3):607-613. doi:10.1016/0092-8674(91)90244-S
38. Cocquerelle C, Mascrez B, Hetuin D, Bailleul B. Mis-splicing yields circular RNA molecules. *FASEB J*. 1993;7(1):155-160. doi:10.1096/fasebj.7.1.7678559
39. Capel B, Swain A, Nicolis S, et al. Circular transcripts of the testis-determining gene Sry in adult mouse testis. *Cell*. 1993;73(5):1019-1030. doi:10.1016/0092-8674(93)90279-Y
40. Ye C-Y, Chen L, Liu C, Zhu Q-H, Fan L. Widespread noncoding circular RNAs in plants. *New Phytol*. 2015;208(1):88-95. doi:10.1111/nph.13585
41. Salzman J, Gawad C, Wang PL, Lacayo N, Brown PO. Circular RNAs are the predominant transcript isoform from hundreds of human genes in diverse cell types. *PLoS One*. 2012;7(2). doi:10.1371/journal.pone.0030733
42. Mortazavi A, Williams BA, McCue K, Schaeffer L, Wold B.

Mapping and quantifying mammalian transcriptomes by RNA-Seq. *Nat Methods*. 2008;5(7):621-628. doi:10.1038/nmeth.1226

43. Jeck WR, Sorrentino JA, Wang K, et al. Jeck, W. R., Sorrentino, J. A., Wang, K., Slevin, M. K., Burd, C. E., Liu, J., … Sharpless, N. E. (2013). Circular RNAs are abundant, conserved, and associated with ALU repeats. RNA, 19(2), 141–157. https://doi.org/10.1261/rna.035667.112Circular RNAs are . *RNA*. 2013;19(2):141-157. doi:10.1261/rna.035667.112
44. Schwanhüusser B, Busse D, Li N, et al. Global quantification of mammalian gene expression control. *Nature*. 2011;473(7347):337-342. doi:10.1038/nature10098
45. Suzuki H, Zuo Y, Wang J, Zhang MQ, Malhotra A, Mayeda A. Characterization of RNase R-digested cellular RNA source that consists of lariat and circular RNAs from pre-mRNA splicing. *Nucleic Acids Res*. 2006;34(8). doi:10.1093/nar/gkl151
46. Ashwal-Fluss R, Meyer M, Pamudurti NR, et al. CircRNA Biogenesis competes with Pre-mRNA splicing. *Mol Cell*. 2014;56(1):55-66. doi:10.1016/j.molcel.2014.08.019
47. Jeck WR, Sorrentino JA, Wang K, et al. Circular RNAs are abundant, conserved, and associated with ALU repeats. *RNA*. 2013;19(2):141-157. doi:10.1261/rna.035667.112
48. Starke S, Jost I, Rossbach O, et al. Exon circularization requires canonical splice signals. *Cell Rep*. 2015;10(1):103-111. doi:10.1016/j.celrep.2014.12.002
49. Barrett SP, Wang PL, Salzman J. Circular RNA biogenesis can proceed through an exon-containing lariat precursor. *Elife*. 2015;4(JUNE):1-18. doi:10.7554/eLife.07540
50. Wilusz JE. A 360° view of circular RNAs: From biogenesis to functions. *Wiley Interdiscip Rev RNA*. 2018;9(4):1-17. doi:10.1002/wrna.1478
51. Ivanov A, Memczak S, Wyler E, et al. Analysis of intron sequences reveals hallmarks of circular RNA biogenesis in animals. *Cell Rep*. 2015;10(2):170-177. doi:10.1016/j.celrep.2014.12.019

52. Zhang XO, Wang H Bin, Zhang Y, Lu X, Chen LL, Yang L. Complementary sequence-mediated exon circularization. *Cell*. 2014;159(1):134-147. doi:10.1016/j.cell.2014.09.001
53. Dubin RA, Kazmi MA, Ostrer H. Inverted repeats are necessary for circularization of the mouse testis Sry transcript. *Gene*. 1995;167(1-2):245-248. doi:10.1016/0378-1119(95)00639-7
54. Piechotta M, Wyler E, Dieterich C, et al. Analysis of Intron Sequences Reveals Hallmarks of Circular RNA Biogenesis in Animals. *Cell Rep*. 2014;10(2):170-177. doi:10.1016/j.celrep.2014.12.019
55. J CS, A PK, John T, et al. The RNA binding protein quaking regulates formation of circRNAs. *Cell*. 2015;160(6). https://www.ncbi.nlm.nih.gov/pubmed/?term=25768908. Accessed October 30, 2019.
56. Errichelli L, Dini Modigliani S, Laneve P, et al. FUS affects circular RNA expression in murine embryonic stem cell-derived motor neurons. *Nat Commun*. 2017;8. doi:10.1038/ncomms14741
57. Barrett SP, Salzman J. Circular RNAs: Analysis, expression and potential functions. *Dev*. 2016;143(11):1838-1847. doi:10.1242/dev.128074
58. Rybak-wolf A, Stottmeister C, Glažar P, et al. Circular RNAs in the Mammalian Brain Are Highly Abundant , Conserved , and Dynamically Expressed Supplemental Figures Figure Sq - related to Figure q.
59. You X, Vlatkovic I, Babic A, et al. Neural circular RNAs are derived from synaptic genes and regulated by development and plasticity. *Nat Neurosci*. 2015;18(4):603-610. doi:10.1038/nn.3975
60. Szabo L, Morey R, Palpant NJ, et al. Statistically based splicing detection reveals neural enrichment and tissue-specific induction of circular RNA during human fetal development. *Genome Biol*. 2015;16(1). doi:10.1186/s13059-015-0690-5
61. Westholm JO, Miura P, Olson S, et al. Genome-wide Analysis of Drosophila Circular RNAs Reveals Their Structural and

Sequence Properties and Age-Dependent Neural Accumulation. *Cell Rep*. 2014;9(5):1966-1980. doi:10.1016/j.celrep.2014.10.062

62. Scarfò R, Legnini I, Peruzzi G, et al. FUS affects circular RNA expression in murine embryonic stem cell-derived motor neurons. *Nat Commun*. 2017;8:14741. doi:10.1038/ncomms14741
63. Huang C, Liang D, Tatomer DC, Wilusz JE. A length-dependent evolutionarily conserved pathway controls nuclear export of circular RNAs. *Genes Dev*. 2018;32(9-10):639-644. doi:10.1101/gad.314856.118
64. Li Z, Huang C, Bao C, et al. Exon-intron circular RNAs regulate transcription in the nucleus. *Nat Struct Mol Biol*. 2015;22(3):256-264. doi:10.1038/nsmb.2959
65. Salzman J, Chen RE, Olsen MN, Wang PL, Brown PO. Cell-Type Specific Features of Circular RNA Expression. *PLoS Genet*. 2013;9(9). doi:10.1371/journal.pgen.1003777
66. Memczak S, Jens M, Elefsinioti A, et al. Circular RNAs are a large class of animal RNAs with regulatory potency. *Nature*. 2013;495(7441):333-338. doi:10.1038/nature11928
67. Bachmayr-Heyda A, Reiner AT, Auer K, et al. Correlation of circular RNA abundance with proliferation - Exemplified with colorectal and ovarian cancer, idiopathic lung fibrosis, and normal human tissues. *Sci Rep*. 2015;5:8057. doi:10.1038/srep08057
68. Du WW, Yang W, Chen Y, et al. Foxo3 circular RNA promotes cardiac senescence by modulating multiple factors associated with stress and senescence responses. *Eur Heart J*. 2017;38(18):1402-1412. doi:10.1093/eurheartj/ehw001
69. Rossi F, Legnini I, Megiorni F, et al. Circ-ZNF609 regulates G1-S progression in rhabdomyosarcoma. *Oncogene*. 2019;38(20):3843-3854. doi:10.1038/s41388-019-0699-4
70. Hansen TB, Wiklund ED, Bramsen JB, et al. miRNA-dependent gene silencing involving Ago2-mediated cleavage of a circular antisense RNA. *EMBO J*. 2011;30(21):4414-4422. doi:10.1038/emboj.2011.359
71. Guo JU, Agarwal V, Guo H, Bartel DP. Expanded

identification and characterization of mammalian circular RNAs. *Genome Biol*. 2014;15(7):1-14. doi:10.1186/s13059-014-0409-z

72. Liu C-X, Li X, Nan F, et al. Structure and Degradation of Circular RNAs Regulate PKR Activation in Innate Immunity. *Cell*. 2019:865-880. doi:10.1016/j.cell.2019.03.046
73. Kristensen LS, Andersen MS, Stagsted LVW, Ebbesen KK, Hansen TB, Kjems J. The biogenesis, biology and characterization of circular RNAs. *Nat Rev Genet*. 2019. doi:10.1038/s41576-019-0158-7
74. Legnini I, Di Timoteo G, Rossi F, et al. Circ-ZNF609 Is a Circular RNA that Can Be Translated and Functions in Myogenesis. *Mol Cell*. 2017;66(1):22-37.e9. doi:10.1016/j.molcel.2017.02.017
75. Yang Y, Fan X, Mao M, et al. Extensive translation of circular RNAs driven by N 6 -methyladenosine. *Cell Res*. 2017;27(5):626-641. doi:10.1038/cr.2017.31
76. Yang Y, Fan X, Mao M, et al. Extensive translation of circular RNAs driven by N6-methyladenosine. *Cell Res*. 2017;27(5):626-641. doi:10.1038/cr.2017.31
77. Zheng Q, Bao C, Guo W, et al. Circular RNA profiling reveals an abundant circHIPK3 that regulates cell growth by sponging multiple miRNAs. *Nat Commun*. 2016;7:1-13. doi:10.1038/ncomms11215
78. Ohler U, Franke V, Moreno-Estelles M, et al. RNA localization is a key determinant of neurite-enriched proteome. *Nat Commun*. 2017;8(1):1-12. doi:10.1038/s41467-017-00690-6
79. Lasda E, Parker R. Circular RNAs co-precipitate with extracellular vesicles: A possible mechanism for circrna clearance. *PLoS One*. 2016;11(2). doi:10.1371/journal.pone.0148407
80. Grottick AJ, Bagnol D, Phillips S, et al. Neurotransmission- and cellular stress-related gene expression associated with prepulse inhibition in mice. *Brain Res Mol Brain Res*. 2005;139(1):153-162. doi:10.1016/j.molbrainres.2005.05.020
81. Lukiw WJ. Circular RNA (circRNA) in Alzheimer's disease

(AD). *Front Genet*. 2013;4(DEC). doi:10.3389/fgene.2013.00307

82. Junn E, Lee K-W, Jeong BS, Chan TW, Im J-Y, Mouradian MM. Repression of alpha-synuclein expression and toxicity by microRNA-7. *Proc Natl Acad Sci U S A*. 2009;106(31):13052-13057. doi:10.1073/pnas.0906277106
83. Mahmoudi E, Fitzsimmons C, Geaghan MP, et al. Circular RNA biogenesis is decreased in postmortem cortical gray matter in schizophrenia and may alter the bioavailability of associated miRNA. *Neuropsychopharmacology*. 2019;44(6):1043-1054. doi:10.1038/s41386-019-0348-1
84. Hanan M, Soreq H, Kadener S. CircRNAs in the brain. *RNA Biol*. 2017;14(8):1028-1034. doi:10.1080/15476286.2016.1255398
85. Venø MT, Venø ST, Rehberg K, et al. Cortical morphogenesis during embryonic development is regulated by miR-34c and miR-204. *Front Mol Neurosci*. 2017;10. doi:10.3389/fnmol.2017.00031
86. Lagier-Tourenne C, Polymenidou M, Cleveland DW. TDP-43 and FUS/TLS: Emerging roles in RNA processing and neurodegeneration. *Hum Mol Genet*. 2010;19(R1):46-64. doi:10.1093/hmg/ddq137
87. Taylor JP, Brown RH, Cleveland DW. Decoding ALS: from genes to mechanism. *Nature*. 2016;539(7628):197-206. doi:10.1038/nature20413
88. Valko K, Ciesla L. Amyotrophic lateral sclerosis. *Prog Med Chem*. 2019;58:63-117. doi:10.1016/bs.pmch.2018.12.001
89. Zou ZY, Zhou ZR, Che CH, Liu CY, He RL, Huang HP. Genetic epidemiology of amyotrophic lateral sclerosis: A systematic review and meta-analysis. *J Neurol Neurosurg Psychiatry*. 2017;88(7):540-549. doi:10.1136/jnnp-2016-315018
90. Ravits J, Appel S, Baloh RH, et al. Deciphering amyotrophic lateral sclerosis: What phenotype, neuropathology and genetics are telling us about pathogenesis. *Amyotroph Lateral Scler Front Degener*. 2013;14(SUPPL1):5-18. doi:10.3109/21678421.2013.778548

91. Droppelmann CA, Campos-Melo D, Ishtiaq M, Volkening K, Strong MJ. RNA metabolism in ALS: when normal processes become pathological. *Amyotroph Lateral Scler Frontotemporal Degener*. 2014;15(5-6):321-336. doi:10.3109/21678421.2014.881377
92. Rosen DR, Siddique T, Patterson D, et al. Mutations in Cu/Zn superoxide dismutase gene are associated with familial amyotrophic lateral sclerosis. *Nature*. 1993;362(6415):59-62. doi:10.1038/362059a0
93. Gerbino V, Carrì MT, Cozzolino M, Achsel T. Mislocalised FUS mutants stall spliceosomal snRNPs in the cytoplasm. *Neurobiol Dis*. 2013;55:120-128. doi:10.1016/j.nbd.2013.03.003
94. Cozzolino M, Pesaresi MG, Gerbino V, Grosskreutz J, Carrì MT. Amyotrophic lateral sclerosis: New insights into underlying molecular mechanisms and opportunities for therapeutic intervention. *Antioxidants Redox Signal*. 2012;17(9):1277-1330. doi:10.1089/ars.2011.4328
95. Kim HJ, Kim NC, Wang Y-D, et al. Mutations in prion-like domains in hnRNPA2B1 and hnRNPA1 cause multisystem proteinopathy and ALS. *Nature*. 2013;495(7442):467-473. doi:10.1038/nature11922
96. Zhao M, Kim JR, Bruggen R van, Park J. RNA-binding proteins in amyotrophic lateral sclerosis. *Mol Cells*. 2018;41(9):818-829. doi:10.14348/molcells.2018.0243
97. Dormann D, Haass C. TDP-43 and FUS : a nuclear affair. 2011;34(7):339-348. doi:10.1016/j.tins.2011.05.002
98. Ragagnin AMG, Shadfar S, Vidal M, Jamali MS, Atkin JD. Motor neuron susceptibility in ALS/FTD. *Front Neurosci*. 2019;13(JUN). doi:10.3389/fnins.2019.00532
99. Deng H, Gao K, Jankovic J. The role of FUS gene variants in neurodegenerative diseases. *Nat Rev Neurol*. 2014;10(6):337-348. doi:10.1038/nrneurol.2014.78
100. Ratti A, Buratti E. Physiological functions and pathobiology of TDP-43 and FUS/TLS proteins. *J Neurochem*. 2016;138 Suppl 1:95-111. doi:10.1111/jnc.13625
101. Baechtold H, Kuroda M, Sok J, Ron D, Lopez BS, Akhmedov

AT. Human 75-kDa DNA-pairing protein is identical to the pro-oncoprotein TLS/FUS and is able to promote D-loop formation. *J Biol Chem*. 1999;274(48):34337-34342. doi:10.1074/jbc.274.48.34337

102. Yang L, Gal J, Chen J, Zhu H. Self-assembled FUS binds active chromatin and regulates gene transcription. *Proc Natl Acad Sci U S A*. 2014;111(50):17809-17814. doi:10.1073/pnas.1414004111
103. Morlando M, Dini Modigliani S, Torrelli G, et al. FUS stimulates microRNA biogenesis by facilitating co-transcriptional Drosha recruitment. *EMBO J*. 2012;31(24):4502-4510. doi:10.1038/emboj.2012.319
104. Rogelj B, Easton LE, Bogu GK, et al. Widespread binding of FUS along nascent RNA regulates alternative splicing in the brain. *Sci Rep*. 2012;2:603. doi:10.1038/srep00603
105. Mastrocola AS, Kim SH, Trinh AT, Rodenkirch LA, Tibbetts RS. The RNA-binding protein fused in sarcoma (FUS) functions downstream of poly(ADP-ribose) polymerase (PARP) in response to DNA damage. *J Biol Chem*. 2013;288(34):24731-24741. doi:10.1074/jbc.M113.497974
106. Fujii R, Takumi T. TLS facilitates transport of mRNA encoding an actin- stabilizing protein to dendritic spines. 2005. doi:10.1242/jcs.02692
107. Fujii R, Okabe S, Urushido T, et al. to Dendritic Spines by mGluR5 Activation and Regulates Spine Morphology. 2005;15:587-593. doi:10.1016/j.cub.2005.01.058
108. Belly A, Moreau-Gachelin F, Sadoul R, Goldberg Y. Delocalization of the multifunctional RNA splicing factor TLS/FUS in hippocampal neurones: Exclusion from the nucleus and accumulation in dendritic granules and spine heads. *Neurosci Lett*. 2005;379(3):152-157. doi:10.1016/j.neulet.2004.12.071
109. Yasuda K, Clatterbuck-Soper SF, Jackrel ME, Shorter J, Mili S. FUS inclusions disrupt RNA localization by sequestering kinesin-1 and inhibiting microtubule detyrosination. *J Cell Biol*. 2017;216(4):1015-1034. doi:10.1083/jcb.201608022
110. Colombrita C, Onesto E, Megiorni F, et al. TDP-43 and FUS

RNA-binding proteins bind distinct sets of cytoplasmic messenger RNAs and differently regulate their post-transcriptional fate in motoneuron-like cells. *J Biol Chem*. 2012;287(19):15635-15647. doi:10.1074/jbc.M111.333450

111. Deshpande D, Higelin J, Schoen M, et al. Synaptic FUS Localization During Motoneuron Development and Its Accumulation in Human ALS Synapses. 2019;13(June):1-17. doi:10.3389/fncel.2019.00256
112. Tischbein M, Baron DM, Lin Y-C, et al. The RNA-binding protein FUS/TLS undergoes calcium-mediated nuclear egress during excitotoxic stress and is required for GRIA2 mRNA processing. *J Biol Chem*. 2019;294(26):10194-10210. doi:10.1074/jbc.RA118.005933
113. Picchiarelli G, Demestre M, Zuko A, et al. FUS-mediated regulation of acetylcholine receptor transcription at neuromuscular junctions is compromised in amyotrophic lateral sclerosis. *Nat Neurosci*. October 2019. doi:10.1038/s41593-019-0498-9
114. Dadon-Nachum M, Melamed E, Offen D. The "dying-back" phenomenon of motor neurons in ALS. *J Mol Neurosci*. 2011;43(3):470-477. doi:10.1007/s12031-010-9467-1
115. Dormann D, Rodde R, Edbauer D, et al. ALS-associated fused in sarcoma (FUS) mutations disrupt transportin-mediated nuclear import. *EMBO J*. 2010;29(16):2841-2857. doi:10.1038/emboj.2010.143
116. Rhoads SN, Monahan ZT, Yee DS, Shewmaker FP. The Role of Post-Translational Modifications on Prion-Like Aggregation and Liquid-Phase Separation of FUS. *Int J Mol Sci*. 2018;19(3). doi:10.3390/ijms19030886
117. Chiò A, Calvo A, Mazzini L, et al. Extensive genetics of ALS : A population-based study in Italy Extensive genetics of ALS A population-based study in Italy. *Nature*. 1993;362(6415):1983-1989. doi:10.1212/WNL.0b013e3182735d36
118. Kwiatkowski TJ, Bosco DA, LeClerc AL, et al. Mutations in the FUS/TLS gene on chromosome 16 cause familial amyotrophic lateral sclerosis. *Science (80-).*

2009;323(5918):1205-1208. doi:10.1126/science.1166066
119. Dini Modigliani S, Morlando M, Errichelli L, Sabatelli M, Bozzoni I. An ALS-associated mutation in the FUS 3'-UTR disrupts a microRNA-FUS regulatory circuitry. *Nat Commun*. 2014;5:4335. doi:10.1038/ncomms5335
120. De Santis R, Santini L, Colantoni A, et al. FUS Mutant Human Motoneurons Display Altered Transcriptome and microRNA Pathways with Implications for ALS Pathogenesis. *Stem cell reports*. 2017;9(5):1450-1462. doi:10.1016/j.stemcr.2017.09.004
121. Capauto D, Colantoni A, Lu L, et al. A Regulatory Circuitry Between Gria2, miR-409, and miR-495 Is Affected by ALS FUS Mutation in ESC-Derived Motor Neurons. *Mol Neurobiol*. 2018;55(10):7635-7651. doi:10.1007/s12035-018-0884-4
122. Wang W-Y, Pan L, Su SC, et al. Interaction of FUS and HDAC1 regulates DNA damage response and repair in neurons. *Nat Neurosci*. 2013;16(10):1383-1391. doi:10.1038/nn.3514
123. Sánchez-Ramos C, Tierrez A, Fabregat-Andrés O, et al. PGC-1α Regulates translocated in liposarcoma activity: Role in oxidative stress gene expression. *Antioxidants Redox Signal*. 2011;15(2):325-337. doi:10.1089/ars.2010.3643
124. Carrì MT, Valle C, Bozzo F, Cozzolino M. Oxidative stress and mitochondrial damage: Importance in non-SOD1 ALS. *Front Cell Neurosci*. 2015;9(FEB). doi:10.3389/fncel.2015.00041
125. Gerbino V, Carrì MT, Cozzolino M, Achsel T. Mislocalised FUS mutants stall spliceosomal snRNPs in the cytoplasm. *Neurobiol Dis*. 2013;55:120-128. doi:10.1016/j.nbd.2013.03.003
126. Sama RRK, Fallini C, Gatto R, et al. ALS-linked FUS exerts a gain of toxic function involving aberrant p38 MAPK activation. 2017;(January):1-13. doi:10.1038/s41598-017-00091-1
127. Scekic-zahirovic J, Sendscheid O, Oussini H El, et al. Toxic gain of function from mutant FUS protein is crucial to trigger

cell autonomous motor neuron loss. 2016;35(10):1077-1097.
128. Kedersha N, Stoecklin G, Ayodele M, et al. Stress granules and processing bodies are dynamically linked sites of mRNP remodeling 4. 2005;169(6):871-884. doi:10.1083/jcb.200502088
129. Anderson P, Kedersha N. Stress granules: the Tao of RNA triage. *Trends Biochem Sci*. 2008;33(3):141-150. doi:10.1016/j.tibs.2007.12.003
130. Yamasaki S, Stoecklin G, Kedersha N, Simarro M, Anderson P. T-cell Intracellular Antigen-1 (TIA-1) -induced Translational Silencing Promotes the Decay of Selected mRNAs * □. 2007;282(41):30070-30077. doi:10.1074/jbc.M706273200
131. Kedersha NL, Gupta M, Li W, Miller I, Anderson P. RNA-binding proteins TIA-1 and TIAR link the phosphorylation of eIF-2α to the assembly of mammalian stress granules. *J Cell Biol*. 1999;147(7):1431-1441. doi:10.1083/jcb.147.7.1431
132. Wilczynska A, Aigueperse C, Kress M, Dautry F, Weil D. The translational regulator CPEB1 provides a link between dcp1 bodies and stress granules. *J Cell Sci*. 2005;118(5):981-992. doi:10.1242/jcs.01692
133. Stoecklin G, Stubbs T, Kedersha N, et al. MK2-induced tristetraprolin:14-3-3 complexes prevent stress granule association and ARE-mRNA decay. *EMBO J*. 2004;23(6):1313-1324. doi:10.1038/sj.emboj.7600163
134. Stöhr N, Lederer M, Reinke C, et al. ZBP1 regulates mRNA stability during cellular stress. *J Cell Biol*. 2006;175(4):527-534. doi:10.1083/jcb.200608071
135. Khong A, Parker R. MRNP architecture in translating and stress conditions reveals an ordered pathway of mRNP compaction. *J Cell Biol*. 2018;217(12):4124-4140. doi:10.1083/jcb.201806183
136. Khong A, Jain S, Matheny T, Wheeler JR, Parker R. Isolation of mammalian stress granule cores for RNA-Seq analysis Sup (Stress Granule Pellet. *Methods*. 2018;137:49-54. doi:10.1016/j.ymeth.2017.11.012
137. Van Treeck B, Parker R. Emerging Roles for Intermolecular

RNA-RNA Interactions in RNP Assemblies. *Cell*. 2018;174(4):791-802. doi:10.1016/j.cell.2018.07.023
138. Souquere S, Mollet S, Kress M, Dautry F, Pierron G, Weil D. Unravelling the ultrastructure of stress granules and associated P-bodies in human cells. *J Cell Sci*. 2009;122(20):3619-3626. doi:10.1242/jcs.054437
139. Hubstenberger A, Courel M, Bénard M, et al. P-Body Purification Reveals the Condensation of Repressed mRNA Regulons. *Mol Cell*. 2017;68(1):144-157.e5. doi:10.1016/j.molcel.2017.09.003
140. Protter DSW, Parker R. Principles and Properties of Stress granules. 2017;26(9):668-679. doi:10.1016/j.tcb.2016.05.004.Principles
141. Rhoads SN, Monahan ZT, Yee DS, Shewmaker FP. The Role of Post-Translational Modifications on Prion-Like Aggregation and Liquid-Phase Separation of FUS. *Int J Mol Sci*. 2018;19(3). doi:10.3390/ijms19030886
142. Shelkovnikova TA, Robinson HK, Southcombe JA, Ninkina N, Buchman VL. Multistep process of FUS aggregation in the cell cytoplasm involves RNA-dependent and RNA-independent mechanisms. *Hum Mol Genet*. 2014;23(19):5211-5226. doi:10.1093/hmg/ddu243
143. Murthy AC, Dignon GL, Kan Y, et al. Molecular interactions underlying liquid−liquid phase separation of the FUS low-complexity domain. *Nat Struct Mol Biol*. 2019;26(7):637-648. doi:10.1038/s41594-019-0250-x
144. Molliex A, Temirov J, Lee J, et al. Phase Separation by Low Complexity Domains Promotes Stress Granule Assembly and Drives Pathological Fibrillization. *Cell*. 2015;163(1):123-133. doi:10.1016/j.cell.2015.09.015
145. Uhlen M, Fagerberg L, Hallstrom BM, et al. Building Predictive Models inRUsing thecaretPackage. *Nucleic Acids Res*. 2011;43(1):462-464. doi:10.1016/j.cell.2010.09.001
146. Andersson MK, Ståhlberg A, Arvidsson Y, et al. The multifunctional FUS, EWS and TAF15 proto-oncoproteins show cell type-specific expression patterns and involvement in cell spreading and stress response. *BMC Cell Biol*. 2008;9.

doi:10.1186/1471-2121-9-37
147. Shelkovnikova TA. Modelling FUSopathies: Focus on protein aggregation. *Biochem Soc Trans*. 2013;41(6):1613-1617. doi:10.1042/BST20130212
148. Sama RR anjit. K, Ward CL, Bosco DA. Functions of FUS/TLS from DNA repair to stress response: implications for ALS. *ASN Neuro*. 2014;6(4). doi:10.1177/1759091414544472
149. Lenzi J, Santis R De, Turris V De, et al. ALS mutant FUS proteins are recruited into stress granules in induced Pluripotent Stem Cells (iPSCs) derived motoneurons Accepted manuscript. 2015;(April). doi:10.1242/dmm.020099
150. Lanson NA, Maltare A, King H, et al. Als mutations in FUS cause neuronal dysfunction and death in caenorhabditis elegans by a dominant gain-of-function mechanism. *Hum Mol Genet*. 2010;21(13):4602-4614. doi:10.1093/hmg/dds299
151. Wichterle H, Peljto M. Differentiation of mouse embryonic stem cells to spinal motor neurons. *Curr Protoc Stem Cell Biol*. 2008;(SUPPL. 5). doi:10.1002/9780470151808.sc01h01s5
152. Liang X, Song MR, Xu ZG, et al. Isl1 Is required for multiple aspects of motor neuron development. *Mol Cell Neurosci*. 2011;47(3):215-222. doi:10.1016/j.mcn.2011.04.007
153. Wichterle H, Lieberam I, Porter JA, Jessell TM. Directed Differentiation of Embryonic.pdf. 2002;110:385-397. doi:10.1016/S0092-8674(02)00835-8
154. Bharadwaj A, Bydoun M, Holloway R, Waisman D. Annexin A2 heterotetramer: Structure and function. *Int J Mol Sci*. 2013;14(3):6259-6305. doi:10.3390/ijms14036259
155. Podbregar M, Mars T, Darovic S, et al. Modelling FUS Mislocalisation in an In Vitro Model of Innervated Human Muscle. *J Mol Neurosci*. 2017;62(3-4):318-328. doi:10.1007/s12031-017-0940-y
156. Khong A, Matheny T, Jain S, et al. The Stress Granule Transcriptome Reveals Principles of mRNA Accumulation in Stress Granules Resource The Stress Granule Transcriptome Reveals Principles of mRNA Accumulation in Stress Granules. *Mol Cell*. 2017;68(4):808-820.e5.

doi:10.1016/j.molcel.2017.10.015
157. Niaki AG, Sarkar J, Cai X, et al. Loss of Dynamic RNA Interaction and Aberrant Phase Separation Induced by Two Distinct Types of ALS/FTD-Linked FUS Mutations. *Mol Cell*. 2019:1-13. doi:10.1016/j.molcel.2019.09.022
158. Luo Y, Na Z, Slavoff SA. P-Bodies: Composition, Properties, and Functions. *Biochemistry*. 2018;57(17):2424-2431. doi:10.1021/acs.biochem.7b01162
159. Abdelmohsen K, Panda AC, Munk R, et al. Identification of HuR target circular RNAs uncovers suppression of PABPN1 translation by CircPABPN1. *RNA Biol*. 2017;14(3):361-369. doi:10.1080/15476286.2017.1279788
160. Kristensen LS, Hansen TB, Venø MT, Kjems J. Circular RNAs in cancer: opportunities and challenges in the field. *Oncogene*. 2018;37(5):555-565. doi:10.1038/onc.2017.361
161. El-Tahir HM, Abouzied MM, Gallitzendoerfer R, Gieselmann V, Franken S. Hepatoma-derived growth factor-related protein-3 interacts with microtubules and promotes neurite outgrowth in mouse cortical neurons. *J Biol Chem*. 2009;284(17):11637-11651. doi:10.1074/jbc.M901101200
162. Marubuchi S, Okuda T, Tagawa K, et al. Hepatoma-derived growth factor, a new trophic factor for motor neurons, is up-regulated in the spinal cord of PQBP-1 transgenic mice before onset of degeneration. *J Neurochem*. 2006;99(1):70-83. doi:10.1111/j.1471-4159.2006.04021.x
163. Tian W, Yan P, Xu N, et al. The HRP3 PWWP domain recognizes the minor groove of double-stranded DNA and recruits HRP3 to chromatin. *Nucleic Acids Res*. 2019;47(10):5436-5448. doi:10.1093/nar/gkz294
164. Raj A, van den Bogaard P, Rifkin SA, van Oudenaarden A, Tyagi S. Imaging individual mRNA molecules using multiple singly labeled probes. *Nat Methods*. 2008;5(10):877-879. doi:10.1038/nmeth.1253
165. Schober P, Schwarte LA. Correlation coefficients: Appropriate use and interpretation. *Anesth Analg*. 2018;126(5):1763-1768. doi:10.1213/ANE.0000000000002864

166. Maddalo D, Manchado E, Concepcion CP, et al. In vivo engineering of oncogenic chromosomal rearrangements with the CRISPR/Cas9 system. *Nature*. 2014;516(7531):423-427. doi:10.1038/nature13902
167. Cong L, Zhang F. Genome engineering using crispr-cas9 system. *Chromosom Mutagen Second Ed*. 2014;8(11):197-217. doi:10.1007/978-1-4939-1862-1_10
168. De Santis R, Alfano V, de Turris V, et al. Mutant FUS and ELAVL4 (HuD) Aberrant Crosstalk in Amyotrophic Lateral Sclerosis. *Cell Rep*. 2019;27(13):3818-3831.e5. doi:10.1016/j.celrep.2019.05.085
169. Zhao S, Jiang E, Chen S, et al. PiggyBac transposon vectors: The tools of the human gene encoding. *Transl Lung Cancer Res*. 2016;5(1):120-125. doi:10.3978/j.issn.2218-6751.2016.01.05
170. McHugh CA, Guttman M. RAP-MS: A Method to Identify Proteins that Interact Directly with a Specific RNA Molecule in Cells. *Methods Mol Biol*. 2018;1649:473-488. doi:10.1007/978-1-4939-7213-5_31
171. Bolger AM, Lohse M, Usadel B. Trimmomatic: A flexible trimmer for Illumina sequence data. *Bioinformatics*. 2014;30(15):2114-2120. doi:10.1093/bioinformatics/btu170
172. Dobin A, Gingeras TR. Mapping RNA-seq Reads with STAR. *Curr Protoc Bioinforma*. 2015;51:11.14.1-11.14.19. doi:10.1002/0471250953.bi1114s51
173. Barnett DW, Garrison EK, Quinlan AR, Stŕmberg MP, Marth GT. Bamtools: A C++ API and toolkit for analyzing and managing BAM files. *Bioinformatics*. 2011;27(12):1691-1692. doi:10.1093/bioinformatics/btr174
174. Quinlan AR, Hall IM. BEDTools: A flexible suite of utilities for comparing genomic features. *Bioinformatics*. 2010;26(6):841-842. doi:10.1093/bioinformatics/btq033
175. Cong L, Zhang F. Genome engineering using crispr-cas9 system. In: *Chromosomal Mutagenesis: Second Edition*. Springer Fachmedien; 2014:197-217. doi:10.1007/978-1-4939-1862-1_10
176. Mehdipour M, Skinner C, Li S, et al. Nanoparticle delivery of

Cas9 ribonucleoprotein and donor DNA in vivo induces homology-directed DNA repair. *Nat Biomed Eng*. 2017;1(11):889-901. doi:10.1038/s41551-017-0137-2

LIST OF PUBLICATIONS

Exploring the regulatory role of circular RNAs in neurodegenerative disorders
Eleonora D'Ambra [1,2], Capauto Davide [2] and Mariangela Morlando
International Journal of Molecular Sciences, 4 Nov 2019;20(21). pii: E5477. doi: 10.3390/ijms20215477.

Amyotrophic lateral sclerosis and denervation alter sphingolipids and up-regulate glucosylceramide synthase
Henriques A, Croixmarie V, Priestman DA, Rosenbohm A, Dirrig-Grosch S, D'Ambra E, Huebecker M, Hussain G, Boursier-Neyret C, Echaniz-Laguna A, Ludolph AC, Platt FM, Walther B, Spedding M, Loeffler JP, Gonzalez De Aguilar JL.
Human Molecular Genetics, Volume 24, Issue 25, 20 December 2015, Pages 7390–7405*2015*

CircRNA localization is altered in FUS mutated motoneurons upon oxidative stress treatment
D'Ambra et al., in preparation